DOE/ER/13251--T3

Progress Report
1984 - 1986

DE-FG03-84ER

DOE/ER/13251--T3

DE92 003464

U.S. DEPARTMENT OF ENERGY

Proposed Research

Received by OSTI

NOV 12 1991

Energy Transfer Processes in Solar Energy Conversion

Michael D. Fayer
Department of Chemistry
Stanford University
Stanford, California 94305

November 1986

DISCLAIMER

This report was prepared as an account of work sponsored by an agency of the United States Government. Neither the United States Government nor any agency thereof, nor any of their employees, makes any warranty, express or implied, or assumes any legal liability or responsibility for the accuracy, completeness, or usefulness of any information, apparatus, product, or process disclosed, or represents that its use would not infringe privately owned rights. Reference herein to any specific commercial product, process, or service by trade name, trademark, manufacturer, or otherwise does not necessarily constitute or imply its endorsement, recommendation, or favoring by the United States Government or any agency thereof. The views and opinions of authors expressed herein do not necessarily state or reflect those of the United States Government or any agency thereof.

MASTER

DISTRIBUTION OF THIS DOCUMENT IS UNLIMITED

Energy Transfer Processes in Solar Energy Conversion

Renewal Research Proposal (Grant: DE-FG03-84ER13251)

M. D. Fayer
Department of Chemistry, Stanford University
Stanford, CA 94305

I. Introduction

Investigations of fundamental aspects of energy transfer processes, particularly electronic excitation transport and electron transfer, in disordered and finite volume systems are described. This proposal represents a continuation and extention of our very successful research in these areas over the past several years. By combining picosecond optical experiments and detailed statistical mechanics theory we will continue to increase our understanding of the complex interplay of structure and dynamics in important energy tranfer situations. A number of different types of problems will be focused on experimentally and theoretically. They are excitation transport among chromophores attached to finite size polymer coils; excitation transport among chromophores in monolayers, bilayers, and finite and infinite stacks of layers; excitation transport in large vesicle systems; and photoinduced electron transfer in glasses and liquids, focusing particularly on the back transfer of the electron from the photogenerated radical anion to the radical cation.

The dynamics of excitation transport in disordered systems is extremely complex because of the distribution of intermolecular seperations which results in a wide distribution of transfer rates and an infinite number of transport pathways. The nature of excitation transport among chromophores (donors) distributed randomly in solution is a classic problem treated by Förster almost 40 years ago [1]. Förster simplified the complex problem of the disordered system by taking the donors to be equally

spaced at the average spacing for a given donor concetration. Excitation transport within this approximation was shown to be diffiusive, i.e., the mean-squared-displacement of the excitation increases linearly in time. However, work in the last few years has shown that this is not an accurate description of excitation transport dynamics in infinite random solutions. Transport is not diffusive [2,3]. Picosecond fluorescence mixing experiments on dye molecules in solution demonstrated that recent theoretical advances provide an accurate and comprehensive description of excitation transport and trapping [4-6]. The theoretical approach is very powerful and has been extended to a variety of other problems [7-9].

The understanding of random solution systems set the stage for the investigation of more complex spatial distributions of chromophores. An area of particular interest is clustered chromophore systems. In such a system molecules are not randomly distributed in space but are constrained to be in some small finite volume. This can lead to very efficient excitation transport, such as that which occurs among chlorophyll molecules in a photosynthetic unit. However, clustered finite volume systems add complexity to the problem of understanding excitation transport in two ways. First, in an infinite volume, the ensemble average of configurations about any starting point is the same, i.e., there is translational invariance of the ensemble average of configuration about any point of initial excitation. In a finite volume this translational invariance is lost. For example, for molecules distributed in a spherical volume, a position of initial excitation near the center of the sphere is very different then an initial excitation near the surface of the sphere [10]. Therefore an average over all starting points as well as all possible configurations about a starting point must be performed. Second, the particular spatial distribution of chromophores must be properly included

in the calculation, i.e., many systems are not characterized by random molecular distributions. A very simple finite volume system, molecules randomly distributed on the surface of a small sphere, was treated in detail both experimentally and theoretically. The system involved dye molecules on the surfaces of spherical micelles [11].

Recently we began to address the problem of chromophores attached to the backbone of finite size polymer coils. This represents a much more complex problem then the micelle problem. Polymer coils have a vast number of configurations. The segments of a coil have a Gaussian pair correlation function for flexible coils, and therefore chromophores randomly tagged on a coil in moderate to low concentration will have an essentially Gaussian distribution in a finite volume. The possible configurations of the coil must be accounted for, and the location of the initial excitation on the coil must be averaged over. Initial attempts to deal with this problem met with some success [12,9,13]. However, early experiments showed that the theories were not in quantitative agreement with experiment [14]. This will be discussed in more detail in Section III, but the problem was that the mathematical complexity of the theories was so great that it was impossible to include accurate descriptions of the chromophore distribution function. In the last few months we have developed a new theoretical approach which is mathematically straightforward enough to permit accurate descriptions of excitation transport for systems with complex topologies [15]. Initial experiments [16] discussed in Section III demonstrate the utility of the approach.

Systems of chromophores attached to polymers are extremely interesting, and understanding excitation transport in such systems is of fundamental importance. By changing the host medium for a coil, the coil

can be made to expand or contract. This change in size for a given coil causes large changes in the rate of excitation transport. In polymer blend systems (one type of coil containing chromophores in another polymer without chromophores) the tagged coils can be isolated or phase separation can occur. In a phase separated system, the tagged coils will separate into microdomains. These microdomains will be inclusions with very high chromophore concentrations in the bulk plastic. We are now positioned, with experiment and theory, to begin to understand such complex systems.

Another class of excitation transport problems involves molecules randomly distributed, but not in three dimensions. These systems, which are discussed in detail in Section IV, are layered systems, including monolayers, bilayers, a finite stack of layers, and an infinite stack of layers. Large vesicles containing chromophores are closely related systems. In a monolayer, chromophores are randomly distributed in two dimensions. A number of years ago we solved this problem theoretically [17] using the same type of infinite order diagrammatic density expansion that worked so successfully for random three dimensional solutions. This theory has been successfully applied to excitation transport among molecules in submonolayer concentrations on the surfaces of solid substrates [18]. However, like in the polymer problem, the theoretical treatment proved to be too mathematically cumbersome to apply to the more complex layered systems. We recently developed a first order cumulant treatment [19] (also used in the polymer problem) which is both accurate and extendable to the layered systems [20].

In a monolayer, molecules are randomly distributed in a plane. Chromophores at an air-liquid interface or chromophores on a surface are examples of systems which can be described as monolayers. The new theoretical results show that the the dynamics are significantly different

if the chromophores' transition dipoles are constrained to be in the plane rather then assuming an isotropic distribution of orientations. The bilayer problem involves an interplay between excitation transport in the plane that contains the initially excited molecule and interplane transfer. Of course the interplane separation is of key importance, but the possible dipole orientations are also important. In a system of a small number of parallel planes, which plane is initially excited affects the transport dynamics. In a system of an infinite number of planes, the separation between planes relative to the average chromophore concentration in a plane strongly affects the transport characteristics. If the interplane separation becomes very small, the transport approaches that of a three-dimensional system. For very large interplane separations, transport becomes two-dimensional. For intermediate separations, the transport has a fractal like character, being between two and three dimensions in nature.

Bilayers are frequently found in biological systems in the form of membranes. In solution, very large vesicles are essentially bilayers since the radius of curvature becomes so large that on the distance scale of excitation transport the bilayer is effective planar. Multilayered systems such as phospholipid multibilayers can be readily constructed. (The theory can handle unequally spaced systems of layers). In a mutlibilayer system, the phospholipid bilayers are separated by an aqueous layer. This can permit reagents to be moved into and out of the excitation transport system. By changing the length of the lipid and the water content, various interplane spacings can be achieved. Multilamellar vesicles also behave as multibilayers. Experiments on these types of interesting quasi-two-dimensional systems are discussed in Section III.

The third area of investigation involves photo induced electron

transfer and back transfer in electron donor-acceptor systems. Photo induced electron transfer chemical reactiors play key roles in photosynthesis and in electron transfer photochemisrty in solution. In photosynthesis the complex biological structure of donors and acceptors inhibits back transfer following photoinduced electron transfer. However, in solution back transfer is frequently in severe competition with diffusional separation of the radical anion and cation [21]. In a glassy solution of donors and acceptors diffusion is elimenated. A full photo-induced cycle consists of optical excitation of the donor, electron transfer to one of a randomly distributed array of acceptors to form a pair of ground state ions, and finally back transfer of the electron to regenerate the neutral ground state donor and acceptor. The forward transfer problem for randomly distributed acceptors and dilute donors was treated by Inokuti and Hirayama (IH) [22]. The probability of finding the donor excited (the electron has not transferred and fluorescence has not occured) decays nonexponentially and is highly concentration dependent. This process can be studied by time resolved or steady state fluorescence experiments since the electron transfer quenches fluorescence [23,24].

The dynamics of back transfer has not been treated in the literature. Back transfer is not the IH problem. The back transfer does not occur form a donor (the anion) into a random distribution of acceptors. The acceptor is a single cation and its position is not random relative to the anion. Rather the separation of the ion pair has a correlation which is determined by the forward process. Since electron transfer is short range, the back transfer tends to occur among ion pairs which are much closer together than the average distance for the concentrations. To understand the competition between back transfer and diffusional separation in solution it is first necessary to understand this problem. Past experiments have generally

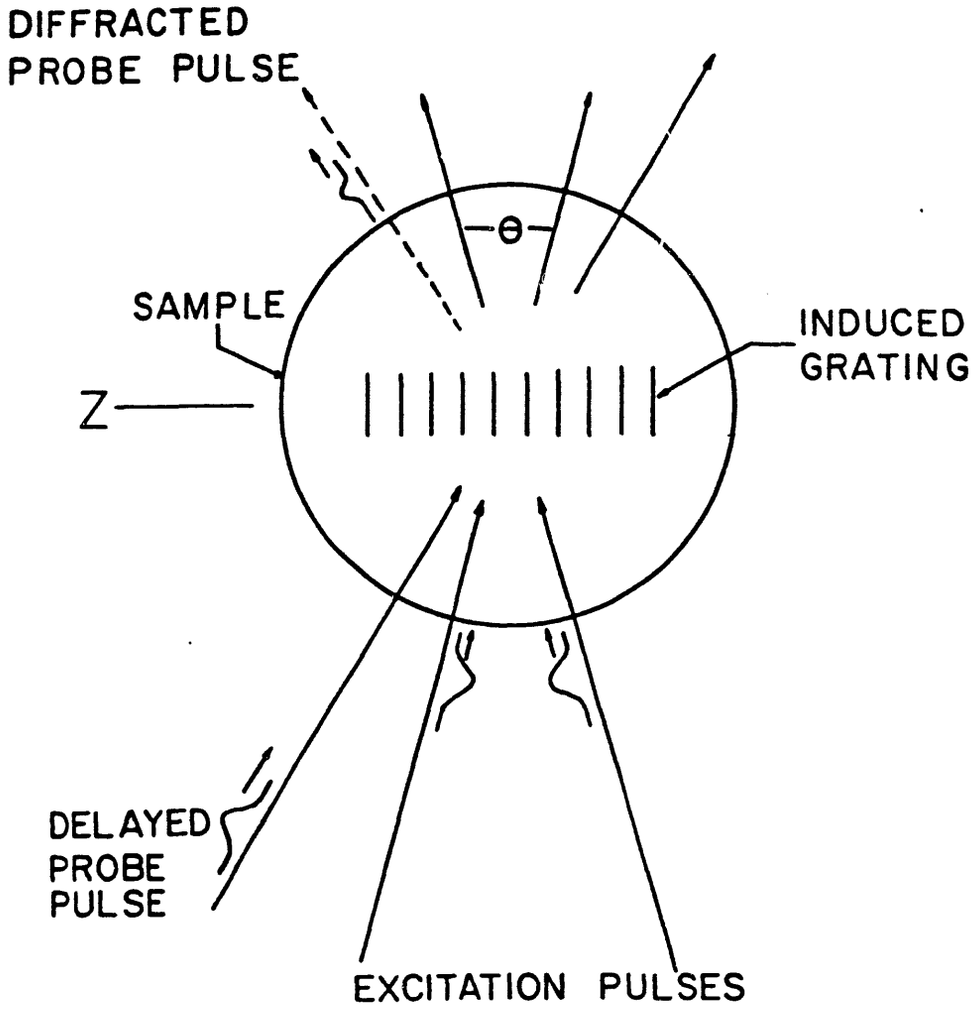

Schematic illustration of the transient grating experiment. Interference between the incoming excitation pulses results in an oscillatory density of excited states, which Bragg-diffracts the subsequent probe pulse. The diffracted probe, which reflects the time evolution of the excited state population, is the signal.

Figure 1

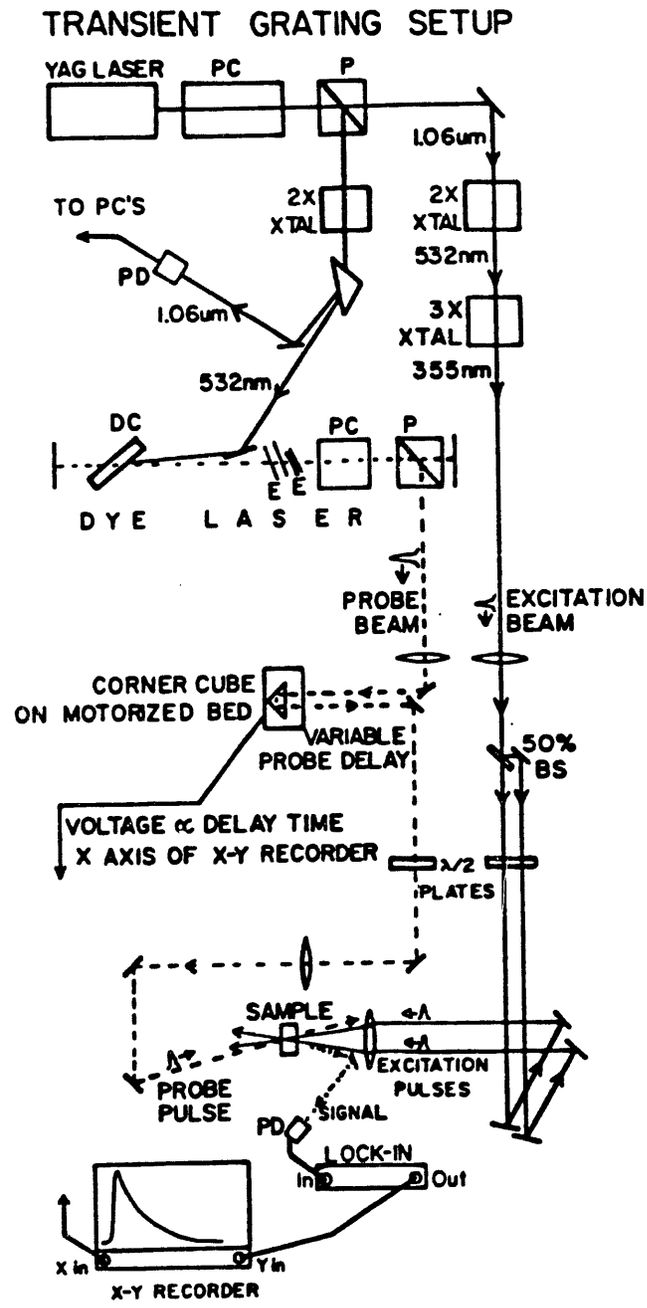

Transient grating experimental setup. A single 1.06 μm pulse is selected from the YAG mode-locked pulse train, frequency tripled to 355 nm, then split into two excitation pulses. These excitation pulses are then recombined at the sample, creating the transient grating. The remainder of the pulse train is frequency doubled to synchronously pump a tunable dye laser whose output probes the grating after a variable delay. The Bragg-diffracted part of the probe pulse is the transient grating signal. PC = Pockels cell; P = polarizer; PD = photodiode; DC = dye cell; E = etalon; BS = beamsplitter.

Figure 2

reflecting polarizer, frequency doubled, and used to synchronously pump a dye laser which is spectrally narrowed and tuned by two intracavity etalons. The dye laser is cavity dumped using another Pockels cell with avalanche transistor driver to give a 20 μJ, 30 ps pulse with a spectral width of 1 cm^{-1}. Both Pockels cells are triggered optically by the IR pulse train to fix the timing between them. The variably delayed dye laser pulse probes the grating at the Bragg angle. The diffracted intensity, measured with a PIN photodiode or a photomultiplier tube and lock-in amplifier, is the signal. In other configurations of the system, the tunable dye pulse is beam split to form the excitation pulses and one of the Nd:YAG harmonics is used as a probe, or the same color is used for both excitation and probing.

A normal population grating is established by the interference of two crossed excitation pulses which have the same polarization. If the polarization of one of the excitation pulses is rotated by 90°, a polarization grating [26] is generated (see Fig. 3). In a normal population grating the two excitation pulses constructively and destructively interfere to produce the optical fringe pattern (Fig. 3b). The interference results from the changing phase relationship of the two overlapping beams along the grating axis (y direction in Fig. 3). When the two pulses have perpendicular polarizations they cannot interfere. However, the two fields will add vectorially. If one pulse is polarized vertically (along x) and the other horizontally (along y), then when their relative phase is 0 (see Fig. 3c) the E-fields will add to give linearly polarized light with a polarization that bisects the vertical and horizontal axes (left side of Fig. 3c). As one moves to the right along the grating axis y, the two pulses are no longer in phase. This results in elliptically polarized light. When the phase difference is $\pi/2$, the light

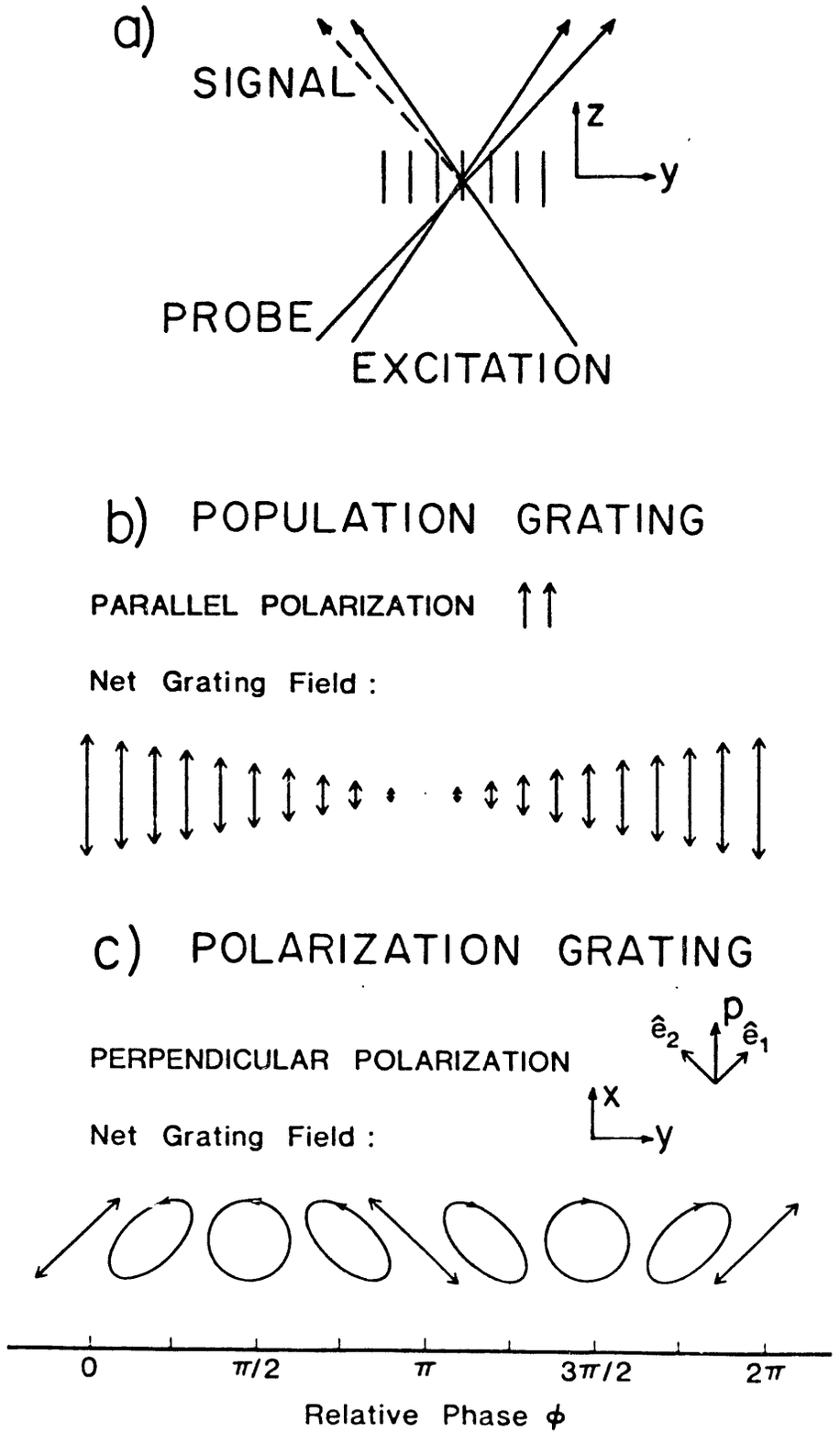
a)
SIGNAL
z
y
PROBE
EXCITATION
b) POPULATION GRATING
PARALLEL POLARIZATION
Net Grating Field :
c) POLARIZATION GRATING
PERPENDICULAR POLARIZATION
p
ê2
ê1
x
y
Net Grating Field :
0
π/2
π
3π/2
2π
Relative Phase φ

Figure 3

is circularly polarized (left circular polarized (lcp) in Fig. 3c). Moving further to the right gives elliptically polarized and then linearly polarized light at a relative phase of π. The linearly polarized light at π is perpendicular to the linearly polarized light at 0. Moving from 0 to π corresponds to one-half a fringe in a normal parallel grating. Continuing to the right the field again becomes elliptical and at $3\pi/2$ it is now right circular polarized (rcp). Finally at 2π, the field is again linearly polarized. Zero to 2π corresponds to one complete fringe in a parallel grating. While the polarization varies from linear to circular to linear for perpendicularly polarized excitation pulses, the total intensity (the absolute value of the electric field squared) is constant everywhere.

The signal in a polarization grating has its polarization rotated 90° relative to the probe polarization when the probe is polarized parallel to one of the excitation polarizations. This results in greatly improved signal to noise since the signal is not only spatially separated from the other pulses but has a distinct polarization. Furthermore, the polarization grating decays with loss of induced polarization in the sample. Thus, it provides a fast time scale alternative to the measurement of fluorescence depolarization (discussed in Sections III and IV). Polarization gratings are also employed for the electron transfer experiments in Section V.

The same type of mode-locked Nd:YAG and dye laser equipment is used in the fluorescence mixing experiments [2,11]. In these experiments, a specific polarization component of the fluorescence decay is directly observed. The setup shown in Fig. 4 is configured for the experiments on excitation transport among dye molecules. (Section IV.) A green single pulse at 532 nm (or a tunable dye laser pulse) excites the sample. The

EXPERIMENTAL SETUP

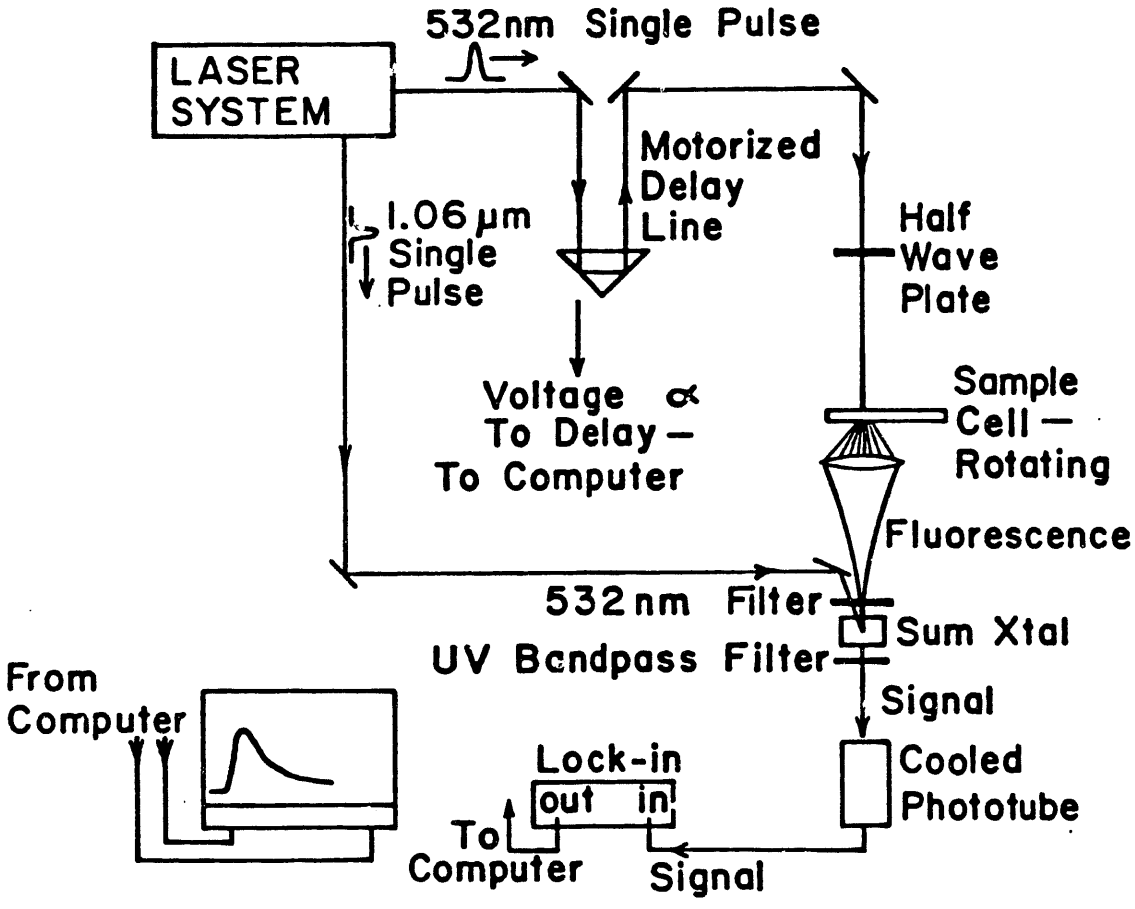

Time resolved fluorescence mixing experimental set up. The laser system consists of a 500 Hz repetition rate, acousto-optically mode-locked and Q-switched Nd:YAG laser. The sample is excited by a 0.532 μ Nd:YAG second harmonic single pulse. The resulting fluorescence which is time coincident in the summing crystal with a 1.06 μ Nd:YAG fundamental pulse is summed to produce a UV signal pulse which is proportional to the fluorescence at that time. The motorized delay line provides temporal resolution by varying the time between the sample excitation and the fluorescence summing.

Figure 4

resulting fluorescence is filtered to remove scattered excitation light and focused into an RDP type-I sum-generating crystal where it overlaps with the path of a 1.06 μm single pulse selected from the YAG laser pulse train by a Pockels cell and polarizer. The fluorescence reaching the sum crystal coincident in time with the 1.06 μm pulse mixes with that pulse to produce a short burst of UV light (~ 365 nm). The UV intensity is proportional to the fluorescence intensity at that time. The sum crystal is oriented so that only the component of the fluorescence polarized parallel to the 1.06 μm polarization is summed. A half-wave plate varies the polarization of the excitation pulse relative to the summing pulse, allowing both the parallel and perpendicular polarization components of the fluorescence ($I_{\parallel}(t)$ and $I_{\perp}(t)$) to be obtained. The excited state lifetime can be determined directly by adjusting the relative polarization of the excitation and summing pulses to the magic angle (54.7°). At this angle, a signal proportional to the total fluorescence is obtained, i.e., depolarization processes do not contribute to the signal.

The time decay is swept out by varying the delay between the excitation pulse and the summing pulse with a motorized delay line. The signal is detected through a UV bandpass filter by a cooled photomultiplier. The phototube output is measured with a lock-in amplifier operating at the laser frequency. The lock-in output and a voltage proportional to the delay time are digitized and stored on disk.

Experiments using conventional detection of time resolved fluorescence, as in some of the polymer experiments discussed in Section III, are performed with the experimental apparatus depicted in Fig. 5.

The frequency doubled (532 nm) output of the acousto-optically mode-locked, Q-switched Nd:YAG laser is used to synchronously pump the dye laser. The dye laser is cavity dumped with a Pockels cell to produce a

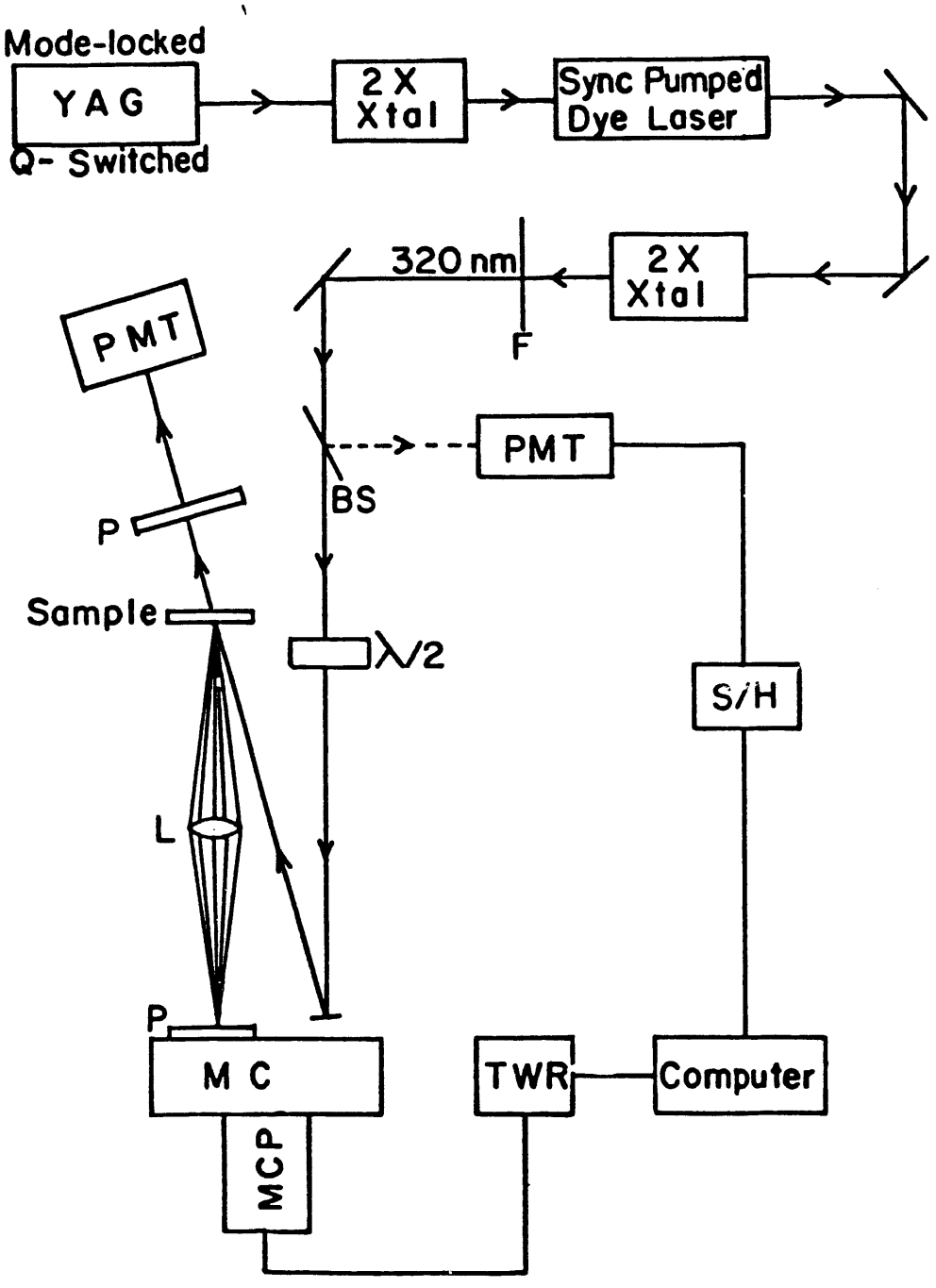

Experimental setup. The output of a mode-locked and Q-switched Nd:YAG laser is frequency doubled and synchronously pumps a dye laser. The dye laser output is doubled to 320 nm for excitation. The polarization of the excitation beam is controlled by a half wave plate. The fluorescence from the sample is collected by a lens, passed through a polarizer and a monochromator, and detected by a multichannel plate coupled to a transient waveform recorder. See text for further details. BS = beam splitter, PMT = photomultiplier tube, λ/2 = half wave plate, S/H = sample and hold circuit, P = polarizer, L = lens, MC = monochromator, MCP = multichannel plate detector, TWR = transient waveform recorder, F = UV transmitting filter, and 2 × Xtal = second harmonic generating crystal.

Figure 5

single pulse at 640 nm which is then frequency doubled to give the ~ 25 psec excitation pulse at 320 nm. A small fraction of each UV excitation pulse is measured with a phototube and sample and hold circuit and recorded by computer so the fluorescence intensity could be normalized to the laser intensity. This eliminates effects due to laser intensity drift. The spot size of the excitation pulse at the sample is of the order of 1 mm and the pulse energies are typically 0.5 to 1 μJoule. The optical density of all samples is ≤ 0.2. No significant readsorption of fluorescence occurs in this O.D. range. The dependence of the recorded fluorescence intensity on the excitation intensity was linear, assuring that the microchannel plate was not saturated and the sample was not being bleached.

Fluorescence from the sample is focused into a monochromator with an interference filter and polarizer on the entrance slit. A microchannel plate (Hamamatsu R1645U-01) coupled to a transient digitizer (Tektronix model R7912) detects the fluorescence at 337 nm. A computer is used to store the fluorescence decays and average many decays to improve signal-to-noise. The time resolution of the detection system is 1.0 nsec.

$I_{\parallel}(t)$ and $I_{\perp}(t)$ are measured by rotating the polarization of the excitation pulse with a half-wave plate and keeping the detector polarizer unchanged at vertical polarization. Since the detection efficiency of the monochromator and microchannel plate can vary with the polarization of the light, thismethod ensures that the absolute ratio of $I_{\parallel}(t)$ to $I_{\perp}(t)$ is preserved.

In addition to checking the birefringence of the samples in a polarizing microscope, the birefringence of the spot actually excited by the laser beam was checked by placing a polarizer and phototube in the excitation beam after the sample and measuring the ratio of the transmitted

light parallel and perpendicular to the incident polarization. This ratio was 200/1 or higher for all samples and is large enough to ensure that there is no distortion in the data due to birefringence in the samples.

III. Excitation Transport in Polymer and Polymer Blend Systems

In this section and Section IV, experiments and theory are described which will increase our understanding of excitation transport in systems with complex spatial distributions of chromophores. Chromophores attached to polymer chains are interesting for a variety of reasons. First, by varying the molecular weight, the number of chromophores per coil, the coil environment, and of course the chemical nature of the coil, a vast number of distinct chromophore spatial distributions can be achieved. This will permit excitation transport experiments and theory to be applied in well defined situations. Second, polymer systems could prove extremely important in practical solar energy conversion schemes. Polymer coils with chromophores can form controlled clustered excitation transport systems, in some sense analogous to photosynthetic antenna complexes. Finally, understanding the dynamics of excitation transport in polymer systems is providing a new and powerful probe of polymer and polymer blend systems. It is straightforward to understand qualitatively the relationship between excitation transport dynamics and the size of an isolated polymer coil which is randomly tagged in low concentration with chromophores. An ensemble of tagged coils in a polymer blend will have some ensemble averaged root-mean-squared radius of gyration, $\langle R_g^2 \rangle^{1/2}$. If in one host $\langle R_g^2 \rangle^{1/2}$ for the guest coils is large because of favorable guest-host thermodynamic interactions, the average distance between chromophores will be large. Since the rate of excitation transport depends on $1/r^6$ where r is the chromophore separation, transport will be slow. If the same guest

polymer is placed in a different host in which the guest-host thermodynamic interactions are less favorable, the coils will contract, and the average chromophore separation will decrease. This decrease will result in more rapid excitation transport. The $1/r^6$ distance dependence makes the excitation transport observables very sensitive to small changes in in the spatial distribution of chromophores.

The accurate description of excitation transport on isolated polymer coils is an interesting and difficult problem. Chromophores attached to a polymer present an inhomogeneous medium for excitation transport. Rather than being randomly distributed, as in a solution, the positions of the chromophores are correlated through the covalent bonds of the polymer. Also, the finite size of the polymer limits the number of sites the excitation can sample. This inhomogeneity in the chromophore distribution resulting from the requirements of polymer chain structure can lead to complicated expressions for the chromophore pair correlation function.

Recently, we have developed a theory for excitation transport on isolated, finite size, flexible polymer coils which contains a reasonable model of the pair correlation function, and which is amenable to the inclusion of any form of the pair correlation function (15). The theory is based on a method developed by Huber [19] for describing excitation transport in infinite, disordered systems. This method has the advantage of being a relatively straightforward time-domain calculation, making the inclusion of different chromophore distribution functions mathematically tractable. The method in general, can be applied to many systems where there are spatial restrictions on and/or correlations between chromophore sites (15,20). The same approach is used in Section IV for the layered systems. Here, we will discuss the application of this theory to

excitation transport among chromophores randomly distributed in moderate concentration on isolated, flexible polymer chains. The theory utilizes a freely jointed chain pair correlation function within a truncated cumulant expansion expression for the excitation transport dynamics.

In systems involving donor-donor excited state transport, the fundamental quantity of theoretical and experimental interest is $G^s(t)$; the ensemble averaged probability that an originally excited chromophore is excited at time t [2]. $G^s(t)$ contains contributions from excitations that never leave the originally excited chromophore, and from excitations that return to the initially excited chromophores after one or more transfer events. $G^s(t)$ does not contain loss of excitation due to lifetime (fluorescence) events.

First, the general method for calculating $G^s(t)$ for any system for which the possible sites of the chromophores are nonequivalent will be outlined. To this point the description is general and also used in Section IV. Then, the necessary equations for treating the problem of isolated polymer chains will be given.

In systems where the chromophore distribution is other than random in an infinite volume, two important points must be taken into account in the calculation of $G^s(t)$, regardless of which formalism is used to describe the transport dynamics. First, in performing the spatial average over all configurations of molecules surrounding the initially excited molecule, the appropriate radial distribution function must be employed. This is true for nonrandom distributions in infinite or finite systems. The second change applies only to finite systems. In an infinite system, the ensemble average over all configurations is translationally invariant. Therefore the average can be performed about any starting point. In a finite system the translational invariance is lost. The ensemble averaged observable

must be calculated for a particular point of initial excitation and then the observable must be averaged over all possible starting locations.

Using the truncated cumulant treatment, first $G_1{}^s(t)$ is found for an initially excited chromophore (labeled 1) fixed in space, averaged over all possible positions of a second chromophore:

$$(1) \qquad \ln G_1^s(t) = \frac{(N-1)}{2A} \int \left[e^{-2\omega_{12}t} - 1 \right] P(r_{12}) d\vec{r}_{12}$$

and where for incoherent, dipole-dipole (Förster type) energy transport with which we are concerned with here,

$$(2) \qquad \omega_{12} = \frac{1}{\tau} \left(\frac{R_0}{r_{12}} \right)^6$$

τ is the fluorescence lifetime and R_0 the critical transfer radius for donor-donor transport [1]. For experiments in high viscosity media, the chromophores are essentially static and the appropriate orientation dependent R_0 must be used [12,13]. N is the number of chromophores in the system. $P(r_{12})d\vec{r}_{12}$ is the probability that there is a chromophore at a distance r_{12} from chromophore 1. The integral is over the physical space and A is the appropriate normalization factor. Next, it is necessary to average over the possible positions of the initially excited chromophore

$$(3) \qquad G^s(t) = \frac{1}{A} \int G_1^s(t) d\vec{r}_1 .$$

For an infinite, disordered system, $P(r_{12})d\vec{r}_{12}$ is $4\pi r_{12}{}^2 dr_{12}$ and Eqs. (1) and (3) become identical to the results of Huber. This cumulant expansion method has been shown to be in excellent agreement with the infinite order diagrammatic theory of Gochanour, Andersen, and Fayer [2] which has been

demonstrated theoretically and experimentally to be an accurate description of energy transport in homogeneous solutions [4,6].

The chromophore concentration is chosen low enough that there is a low probability of having more than one chromophore per statistical segment of the chain. This inhibits the formation of excimer traps which block transport. It also assures that there are no angular correlations among the chromophores' transition dipoles and that transport is three dimensional rather than quasi one dimensional (along the chain backbone). The overall concentration of tagged coils in the blend is taken to be low enough that there is no interchain transfer, i.e., all excitation transfer occurs among chromophores tagged on the same chain.

The forms of Eqs. (1) and (3) permit any model of the polymer pair correlation function to be used in the transport calculation. Here we are considering flexible chains and it is reasonable to use a freely jointed chain model, which obeys Gaussian statistics, in the calculations. The chain segment length is identified with the statistical polymer segment (Kuhn segment) length. In this model, the conformation averaged radial probability of finding any other polymer segment a distance r from a segment i is [27]

$$(4) \qquad p_1(r)d\vec{r} = \frac{4\pi}{(\bar{N}-1)} \sum_{\substack{j=1 \\ j\neq i}}^{\bar{N}} \left(\frac{3}{2\pi a^2|i-j|}\right)^{3/2} \exp\left(\frac{-3r_{12}^2}{2a^2|i-j|}\right) r_{12}^2 dr_{12}$$

where $\bar{N}$ is the number of statistical segments and a is the statistical segment length. Since the chromophore concentration on the chain is small (< 10%) we identify the probability of finding a second chromophore (labeled 2) at a distance r_{12} from an initially excited chromophore (labeled 1) placed on segment i with the probability that there is a

polymer segment at that distance. Replacing r with r_{12} in Eq. (4) (this will be denoted by $p_i(r_{12})$) and multiplying by N - 1 (N is the number of chromophores on the chain) yields the conformation averaged probability of finding another chromophore a distance r_{12} from the initially excited chromophore, excluding the small correction due to additional, unexcited chromophores on segment i.

The correction due to unexcited chromophores on the segment containing the initially excited chromophore, i, can be included by calculating the average number (n) of unexcited chromophores on segment i and using some reasonable chromophore distribution function ($p'(r_{12})$) for this segment. Then the probability of an unexcited chromophore being a distance r_{12} away from the initially excited chromophore on the ith segment is

$$(5) \qquad P_i(r_{12})d\vec{r}_{12} = \left\{ n\, p'(r_{12}) + (-1 - n)\, p_i(r_{12}) \right\} d\vec{r}_{12}$$

For low concentrations of chromophores, n is a small number and the choice of $p'(r_{12})$ is not critical. It is only necessary to concentrate the appropriate chromophore density in the region of space of the ith segment. A simple model for $p'(r_{12})$ is to assume that the initially excited chromophore is in the center of the segment and surrounded by a random distribution of the n chromophores, i.e.,

$$(6) \qquad \begin{aligned} p'(r_{12})d\vec{r}_{12} &= 4\pi r_{12}^2 dr_{12} && 0 \le r_{12} \le a/2 \\ &= 0 && r_{12} \ge a/2 \end{aligned}$$

If Eq. (5) with Eq. (6) is substituted for $(N-1)P(r_{12})d\vec{r}_{12}$ in Eq. (1-3) and the position of the initially excited chromophore is averaged over by summing the equally weighted contributions from each segment i, the expression for $G^s(t)$ is

$$(7) \qquad G^s(t) = \frac{1}{\bar{N}} \sum_{i=1}^{\bar{N}} \left\{ \mathrm{Exp}\left[\frac{4\pi}{2} \int_0^\infty P_i(r_{12}) \left[e^{-2\omega_{12}t} - 1 \right] r_{12}^2 dr_{12} \right] \right\}$$

$G^s(t)$ is directly related to the time-dependent fluorescence anisotropy which can be measured through time-resolved fluorescence depolarization, polarized transient grating or polarized absorption techniques [2,6]. In time-resolved fluorescence depolarization experiments a sample of randomly oriented chromophores is excited by a short pulse of plane polarized light. The decay of the fluorescence intensities polarized parallel ($I_\parallel(t)$) and perpendicular ($I_\perp(t)$) to the exciting light can be written as

$$(8) \qquad \begin{aligned} I_\parallel(t) &= e^{-t/\tau}(1 + 2\, r(t)) \\ I_\perp &= e^{-t/\tau}(1 - r(t)). \end{aligned}$$

τ is the fluorescence life time and $r(t)$ is the time dependent fluorescence anisotropy. $r(t)$ contains information about all sources of depolarization and can be obtained from the individual parallel and perpendicular components of the fluorescence intensity. From Eq. (8)

$$(9) \qquad r(t) = \frac{I_\parallel(t) - I_\perp(t)}{I_\parallel(t) + 2\, I_\perp(t)}$$

The initially excited ensemble is polarized along the direction of the excitation $\bar{E}$ field and gives rise to polarized fluorescence. Transport occurs into an ensemble of chromophores with randomly distributed dipole directions and the fluorescence becomes unpolarized. The random distribution is assured by the low concentration of the chromophores. To a slight extent, on the time scale of interest, depolarization also occurs as a result of chromophore motion. In this case the fluorescence anisotropy is

(10) $r(t) = C\,\phi(t)\,G^s(t)$

where $\phi(t)$ is the rotational correlation function which contains the effects due to motion of the chromophores. C is a time-independent constant that describes the degree of polarization of the excitation and emission transitions involved.

In order to obtain $G^s(t)$ for a given polymer, experiments on two different samples must be performed. These samples differ only in that the guest copolymers have a different fraction of chromophore containing monomers. Copolymer A is the polymer of interest and has an appreciable number of chromophores, such that excitation transport will occur. Its fluorescence anisotropy, $r_A(t)$, is given by Eq. (10). Copolymer B has such a small number of chromophores that excitation transport is negligible ($G^s(t) = 1$) and only chromophore motion contributes to the anisotropy,

(11) $P_B(t) = C\,\phi(t)$

$G^s(t)$ arising from the excitation transport on copolymer A can be calculated from the two experimental anisotropies:

(12) $G^s(t) = r_A(t)/r_B(t)$

This method of determining $G^s(t)$ has the advantage that detailed knowledge of the parameters C and $\phi(t)$ is unnecessary.

To obtain a value for $\langle R_g^2\rangle^{1/2}$ of the copolymer A, we compare the experimentally determined $G^s(t)$ to a theoretical calculation of $G^s(t)$ (from Eqs. (4)-(7)) for the same copolymer. Once the molecular weight and number of chromophores are known (these can be independently determined), the theory has only one adjustable parameter; the statistical segment length. This parameter is directly related to $\langle R_g^2\rangle^{1/2}$ by

(13) $\langle R_g^2\rangle = \frac{1}{6}(\bar{N}\,a^2)$

Thus, a fit of the experimentally determined $G^s(t)$ with a theoretically calculated $G^s(t)$ determined by adjusting the statistical segment length will give a measure of $\langle R_g^2 \rangle^{1/2}$ for the copolymer.

Earlier experiments have shown the utility of excitation transport measurements in providing relative information regarding coil size in polymer blends (14). Here, we will summarize the results of recent experiments (16) which demonstrate that monitoring excitation transport on isolated coils in solid blends through time-resolved fluorescence depolarization techniques provides a quantitative measure of $\langle R_g^2 \rangle^{1/2}$ for the guest polymer and therefore demonstrates that the theory provides a quantitative description of excitation transport.

The experiments to date have been performed on PMMA coils tagged with naphthalene chromophores in PMMA as a host material. The tagged coils are copolymers of 2-vinylnaphthalene (2-VN) and methyl methacrylate. Experiments on different molecular weight guest copolymers are necessary to show the general applicability of the theory relating $G^s(t)$ to $\langle R_g^2 \rangle^{1/2}$ and to confirm the utility of assuming a Gaussian segment distribution for PMMA. Since the presence of the naphthalene groups could perturb the average chain conformation, $\langle R_g^2 \rangle^{1/2}$ was determined for a series of copolymers of essentially the same molecular weight but differing in the average number of naphthalenes on the chains.

Since the naphthalene chromophores in the copolymers have a relatively long lifetime (50 nsec), conventional electronic detection of time resolved fluorescence depolarization was employed. The experimental setup is described in Section II. The first experiments were performed on samples made from copolymer 9-23 (0.087 mole fraction 2-VN, 23,400 M_w) and from copolymer 9-60 (0.087 mole fraction 2-VN, 59,800 M_w) in 120,000 M_w PMMA. In both cases, the amount of copolymer in the host polymer was 3/8 weight

percent. Figure 6a shows the polarized fluorescence decays ($I_{\parallel}(t)$ and $I_{\perp}(t)$) for the copolymer 9-23/PMMA blend. Figure 6b (lower curve) shows the fluorescence anisotropy, r(t), calculated from the data, using Eq. (9). Also shown (upper curve) is r(t) obtained in the same manner for a 0.0015 mole fraction 2-VN copolymer (I). This sample contains so few chromophores that depolarization occurs solely as a result of chromophore motion. There is no excitation transport.

As discussed above, to obtain the experimental $G^s(t)$ for copolymer 9-23, it is necessary to take the ratio of the anisotropies of copolymer 9-23 to copolymer I. The resulting experimental $G^s(t)$ curve is shown in Figure 7. Figure 8 shows the experimental $G^s(t)$ obtained in the same manner for copolymer 9-60. In both, we also show the best fits (smooth curves) obtained from the theory described above. Variation of the single adjustable parameter, the statistical segment length a, results in $\langle R_g^2 \rangle^{1/2}$ of 37 ± 3 Å and 61 ± 3 Å for the 23,400 M_w and 59,800 M_w copolymers, respectively. The incredible sensitivity of excitation transport to the spatial distribution of chromophores (coil size) is demonstrated by theoretical curves at ±2 Å from the best fits.

The measured $\langle R_g^2 \rangle^{1/2}$ of these two polymers varies with the square root of the chain length. This is as expected for flexible coils [28] and indicates that the Gaussian segment distribution function utilized in the analysis of the data is applicable to these copolymers. Neutron scattering experiments on isolated PMMA coils in a deuterated PMMA host show this same scaling of $\langle R_g^2 \rangle^{1/2}$ with molecular weight [29].

Since these blends are essentially PMMA in PMMA, the copolymers are approximately in θ-conditions [30]. Assuming that these copolymers are essentially PMMA at θ-conditions, it is possible to compare these results

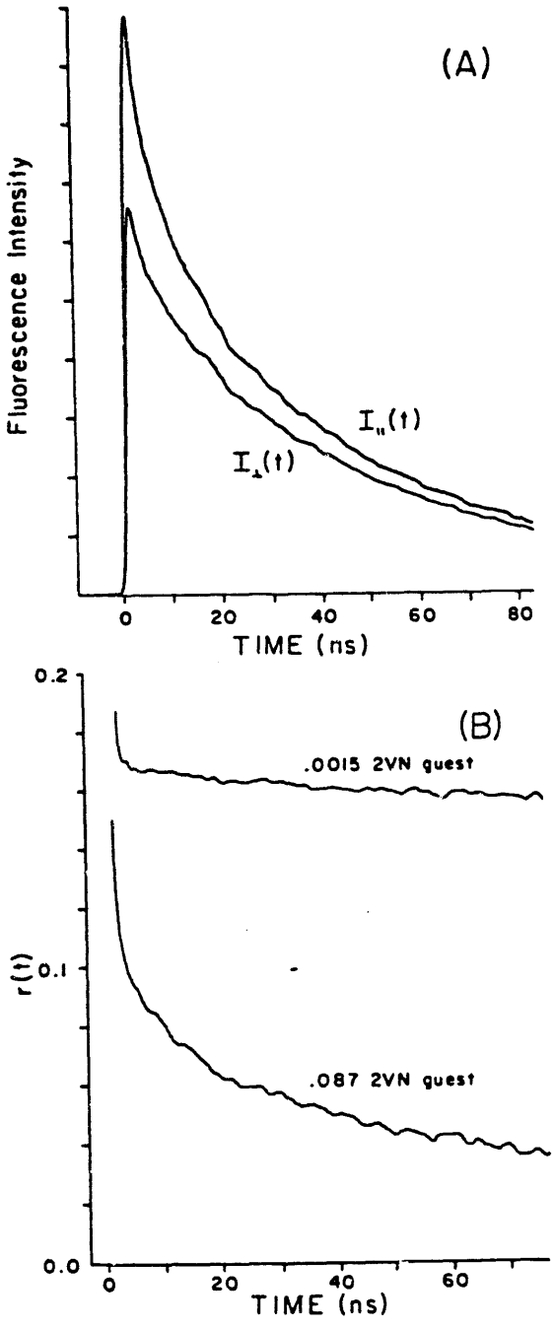

a) Polarized fluorescence decays for detection parallel ($I_{\parallel}(t)$) and perpendicular ($I_{\perp}(t)$) to the excitation polarization. The sample is copolymer 9-23 (23,400 M_w, 0.087 mole fraction 2-VN) in a 120,000 M_w PMMA host. Copolymer concentration is 0.38 wt. percent.

b) Fluorescence anisotropies, r(t), calculated from experimental $I_{\parallel}(t)$ and $I_{\perp}(t)$ (see Eq. 9). The upper curve is a copolymer with a very small mole fraction (0.0015) of 2-vinylnaphthalene (copolymer I). Excitation transport does not occur and the time dependence is due to very slow rotational depolarization. The lower curve is from the data shown in Figure a. Here, the time dependent depolarization is due to both excitation transport and the small amount of rotational depolarization.

Figure 6

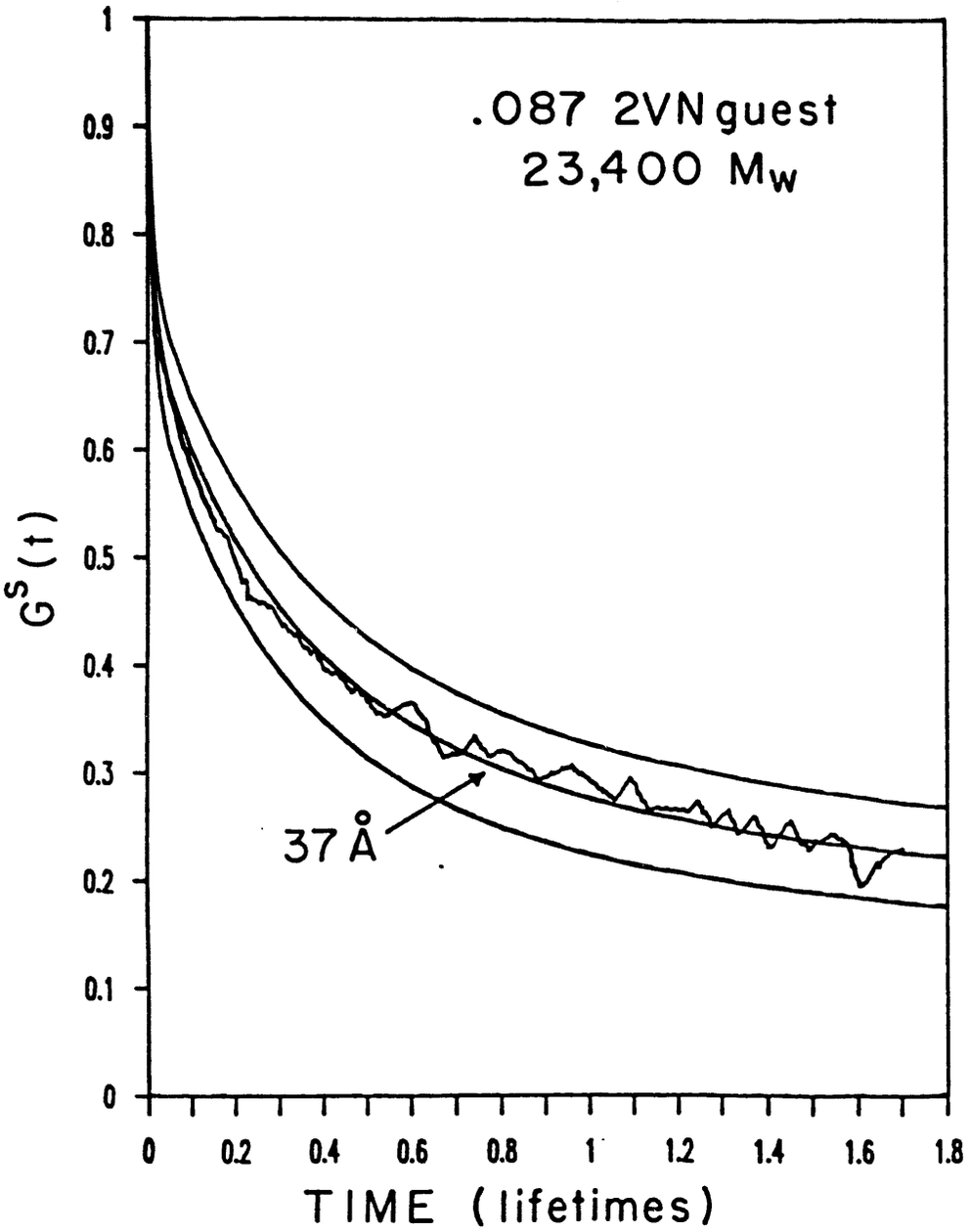

The quantity of experimental and theoretical interest is $G^s(t)$, the ensemble averaged probability that the excitation is on the originally excited chromophore at time t. The experimental $G^s(t)$ results from taking the ratio of the lower to the upper anisotropy curves in Figure 6 b (see Eqs. (10)-(12)). Shown is the experimental $G^s(t)$ for copolymer 9-23 (23,400 M_w, 0.087 mole function 2-VN) in a 120,000 M_w PMMA host. Also shown are theoretical $G^s(t)$ curves calculated using Eq. (7) for a 23,400 M_w PMMA chain with 20 naphthalenes. The best fit, obtained by adjusting the statistical segment length a, results in an $\langle R_g^2 \rangle^{1/2}$ of 37 Å. This result is in close agreement with light scattering determinations of $\langle R_g^2 \rangle^{1/2}$ for a PMMA coil in a θ-condition media. The upper and lower theoretical curves are for 39 Å and 35 Å, respectively.

Figure 7

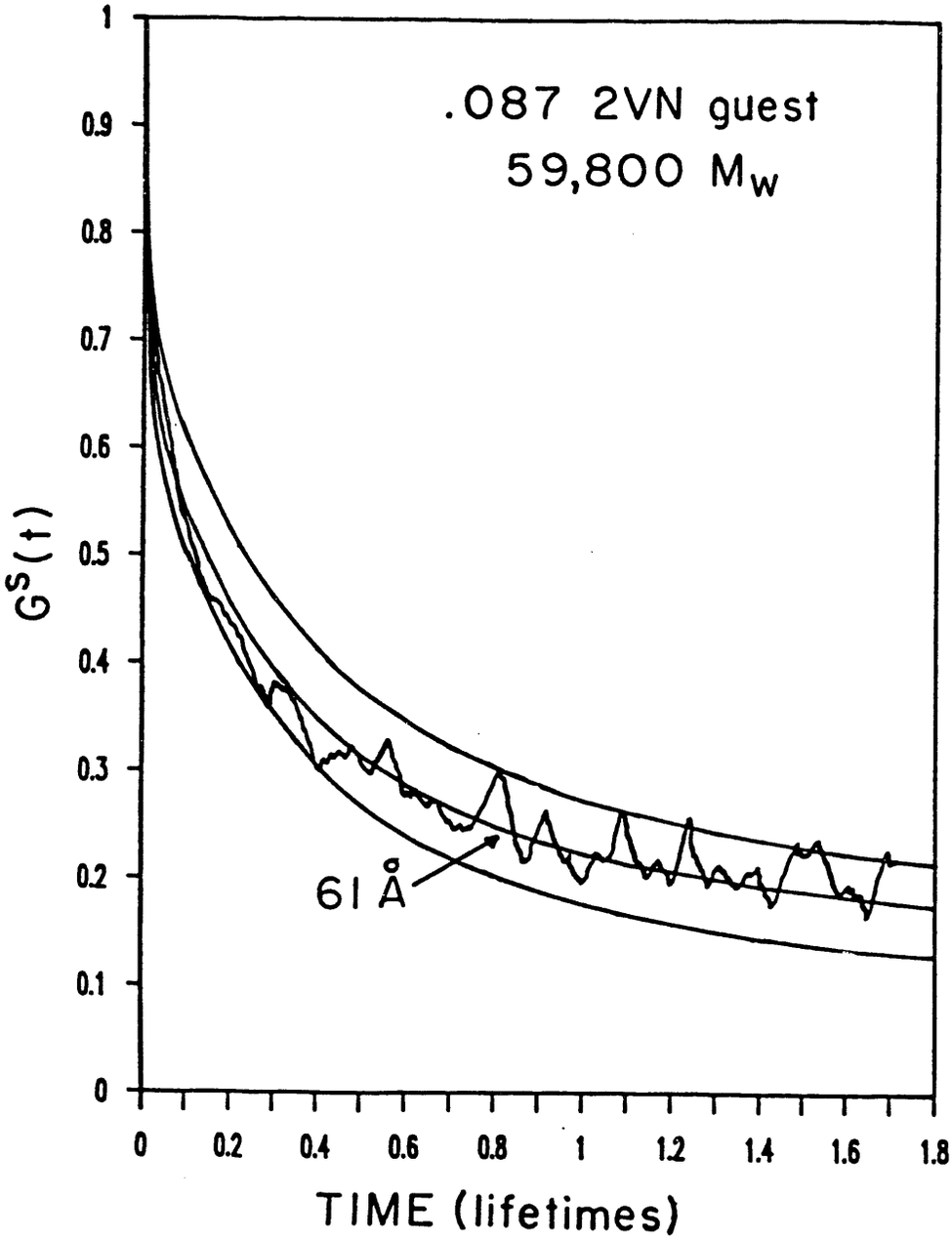

$G^s(t)$, the ensemble averaged probability that the excitation is still on the initially excited molecule. The experimental $G^s(t)$ is for copolymer 9-60 (59,800 M_w, 0.087 mole fraction 2-VN) in a 120,000 M_w PMMA host. Also given are theoretical $G^s(t)$ curves for a 59,800 M_w PMMA chain with 49 naphthalenes. The best fit yields an $\langle R_g^2 \rangle^{1/2}$ of 61 Å. Also given are theoretical curves for 63 Å (upper) and 59 Å (lower). The results are in very good agreement with other methods for determining $\langle R_g^2 \rangle^{1/2}$ of θ-condiion PMMA.

Figure 8

with light scattering measurements of $\langle R_g^2 \rangle^{1/2}$ for equivalent molecular weight PMMA in θ-solvents. The values can be easily caculated from tabulated data [31]. For 23,000 M_w and 60,000 M_w PMMA at θ-condition, $\langle R_g^2 \rangle^{1/2}$ should be 39 ± 4 Å and 64 ± 7 Å, respectively. The results from the excitation transport experiments are in excellent agreement with these values.

Although the results for the two copolymers with 0.087 mole fraction of naphthalene containing monomers agree very well with other determinations of $\langle R_g^2 \rangle^{1/2}$ for θ-condition PMMA, it is important to ascertain that different concentrations of chromophores can be handled with the experiments and theory. This was accomplished by obtaining experimental $G^s(t)$ curves for three copolymers of essentially the same molecular weight, but varying in the amount of naphthalene in the chains. These three copolymers are designated 9-23, 6-22, and 4-23 and contain 8.7, 5.9, and 4.0 mole percent of naphthalene containing monomers, respectively. The samples consisted of 3/8 weight percent of the desired copolymer in the 120,000 M_w host PMMA. Figure 9 shows the experimental $G^s(t)$ curves obtained for these copolymers along with the theoretical best fits. The resulting values for $\langle R_g^2 \rangle^{1/2}$ are 37 ± 3 Å, 39 ± 3 Å, and 38 ± 3 Å for the three copolymers in order from the highest to the lowest naphthalene content. These results are in quantitative agreement with solution $\langle R_g^2 \rangle^{1/2}$ measurements under θ-conditions. In addition, these results indicate that the presence of the naphthalene containing monomers does not significantly perturb the average coil dimensions, at least up to naphthalene concentrations of nine mole percent.

Table I summarizes the results for the various copolymers which have been studied to date. A comment on the error bars associated with the measurements of $\langle R_g^2 \rangle^{1/2}$ in this study is necessary. The theoretical $G^s(t)$

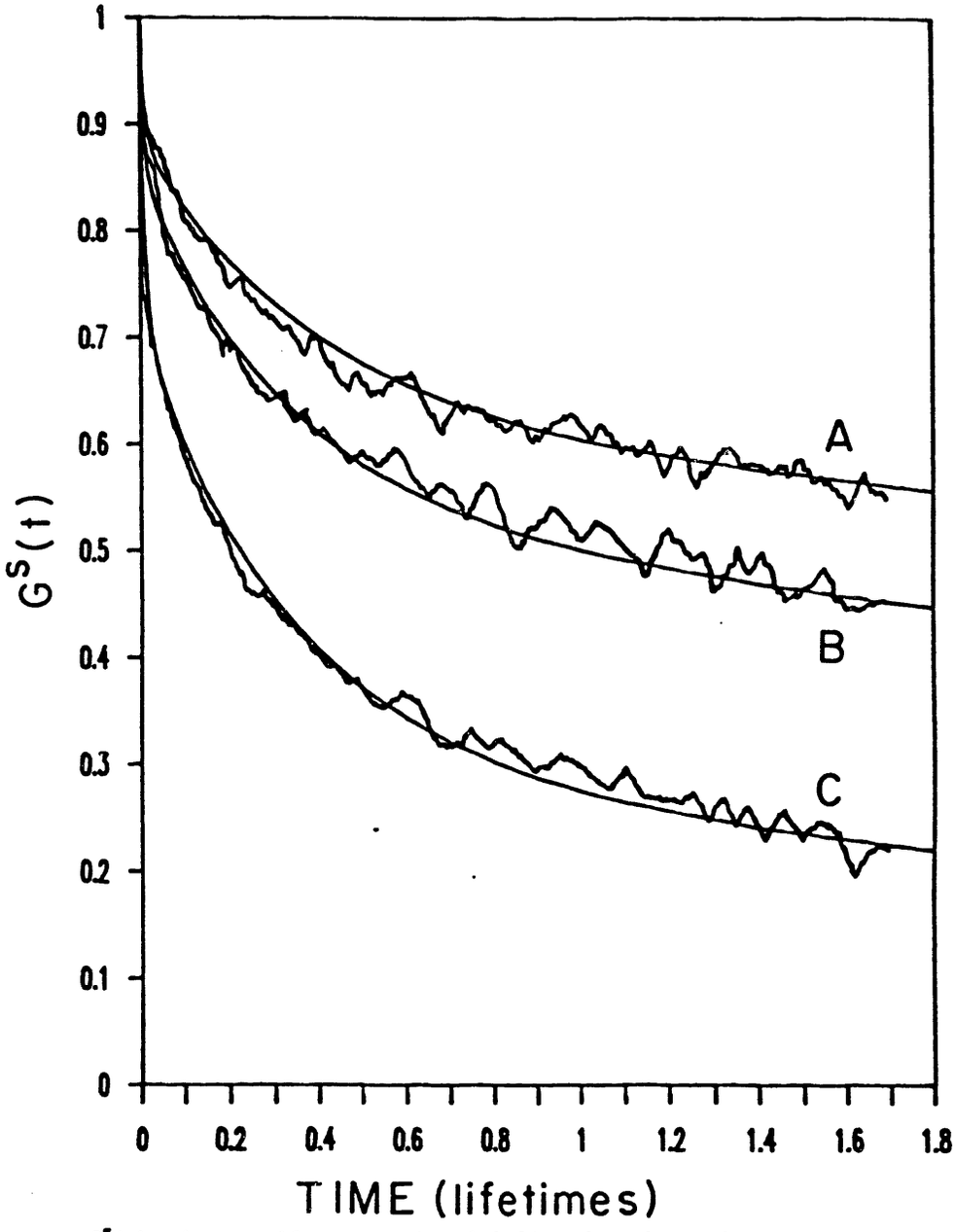

$G^s(t)$, the ensemble averaged probability that the excitation is still on the originally excited chromophore. Data is shown for three copolymers of essentially the same molecular weight but differing in mole fraction of 2-VN. Curve A is copolymer 4-23 (22,700 M_w, 0.04 mole fraction 2-VN), curve B is copolymer 6-22 (22,400 M_w, 0.087 mole fraction 2-VN), and curve C is copolymer 9-23 (23,000 M_w, 0.087 mole fraction 2-VN). Also shown are the best fit theoretical $G^s(t)$ curves for equivalent molecular weight PMMA chains with the appropriate number of naphthalenes. The resulting values for $\langle R_g^2 \rangle^{1/2}$ are 38 Å, 39 Å, and 37 Å in order from A to C. These results show that the presence of the naphthalene containing monomers does not significantly perturb the average chain dimensions at least up to concentrations of 9 mole percent 2-VN.

Figure 9

curves at ±2 Å shown in Figures 7 and 8 are to show the sensitivity of $G^s(t)$ to small changes in $\langle R_g^2 \rangle^{1/2}$. The reported errors in Table I are estimated from errors in the measurement of the average number of naphthalenes per chain and the weight average molecular weight.

TABLE I. Summary of Results

Copolymer	$\langle R_g^2 \rangle^{1/2}$ Determined by Excitation Transport	$\langle R_g^2 \rangle^{1/2}$ for equivalent Light Scattering in θ solvent
4-23	38 ± 3	39 ± 4
6-22	39 ± 3	39 ± 4
9-23	37 ± 3	39 ± 4
9-60	61 ± 3	64 ± 7

The experiments and theory just described represent the first time that a quantitative understanding of excitation transport in a polymer system has been achieved. In fact, these polymers are the most complex structures that have been delt with accurately. We will continue this line of research. First, we will examine a wider variety of molecular weights and chromophore concentrations in the tagged PMMA in PMMA system. Very small coils could require a different pair correlation function since very small coils in principal will not obey Gaussian statistics. As discussed above the formalism can be used with any distribution function for polymer systems and for other types of systems.

The tagged PMMA in PMMA systems are in some sense idealized. They are essentially PMMA in PMMA, and therefore the coils are in a theta condition environment. One of the intriguing things about polymer excitation transport systems is that the same tagged coil, when placed in different environments, will have a different size and therefore a different spatial distribution of chromophores. To obtain a fundamental understanding of the nature of such effects, we will examine a series of blends involving tagged PMMA with polystyrene (PS) and poly(styrene-acrylonitrile) (PSAN). PMMA is

not highly miscible in PS. Therefore the coils should contract dramatically, and the rate of excitation transport should increase significantly. By examining a series of different molecular weight PMMA coils in PS we should be able to develop a detailed understanding of excitation transport in non-theta condition systems. PMMA is highly miscible in PSAN. The tagged PMMA coils will therefore expand beyond their theta condition size. Excitation transport should slow down. By examining tagged PMMA in mixtures of PS and PSAN, a continuous modification of the chromophore distribution function can be obtained. Another system which can be used in a like manner is a copolymer of styrene and methylmethacralyte. With these types of systems we can develop an understanding of tailored clustered chromophore excitation transport systems.

In the experiments described above, the tagged coils will be in relatively low concentration in the host polymer. In systems in which the tagged coils are only moderately miscible, increasing the concentration will lead to phase separation. In a phase separated system the guest coils form microdomains which are rich in the guest coils. This will cluster a large number of the tagged coils in a very small volume, with an associated significant increase in the rate of excitation transport. The detailed nature of the transport in phase separated domains will depend on the structure of the domain. We have a prelimenary result indicating a sudden increase in transport upon phase separation [14]. Using experiments and theory analogous to those described above, we will address the problem of excitation transport in phase separated domains. By controlling the concentration and miscibility of the tagged coils in the host polymer, a very wide range of excitation transport characteristics can be obtained.

To understand the fundamentals of excitation transport in polymer systems, any type of chromophore is useful. However, we do not wish to only examine naphthalene containing systems. We have just begun work on polymers containing pyrene as a chromophore and will expand the work into chromophores which absorb in the visible. The major difficulty is synthesis and characterization. Several of the faculty members at Stanford, who have an interest in polymers, have convinced the Stanford Center for Materials Research (MRL) to obtain polymer preparation and characterization equipment. The first of this equipment (light scattering and chromatographs) has recently arrived. This will be a tremendous aid in preparing new chromophore containing polymer systems.

IV. Layered Excitation Transport Systems

In this section, experiments to investigate excitation transport in layered systems are discussed. We have recently developed the basic theory necessary to begin a detailed understanding of these systems [20]. The theoretical approach involves the same type of cumulant expansion described in Section III. Therefore it will not be repeated here. Essentially, it is necessary to average over the chromophore distribution which is appropriate for the layered systems rather then the tagged polymer chromophore distributions.

Very briefly, a unified treatment of dipole-dipole excitation transfer in disordered systems was developed for the cases of direct trapping (DT) in two-component systems and donor-donor transfer (DD) in one-component systems [20]. Using the cumulant theory first applied by Huber [19] we calculate the configurational average of $G^S(t)$, the probability of finding an initially excited molecule still excited at time t. For the isotropic three-dimentional case treated by Huber excellent correspondence is found

with the previously reported infinite diagrammatic approximation. The anisotropy of the dipole-dipole interaction is included in the averaging procedure. Two regimes of orientational mobility are considered: the dynamic and static limit, rotations being much faster or slower respectively than the energy transfer. The following geometrical distributions are investigated: (a) Infinite systems of one, two, and three dimensions which lead to Förster-like decays. Two orientational distributions are considered for monolayers: dipoles confined to the plane or oriented isotropically. (b) Bilayers and multilayers. The averaging procedure for transfer from one layer to another was developed in detail. The main parameters determining the decay of $G^s(t)$ are the surface concentration and the ratio of the layer separation and the Förster radius. In a stack with a small number of layers, which is a finite system in one of the dimensions, an average over positions of the initially excited donor is included. At low surface concentration the decay gradually changes from two to three dimensional character as one increases the number of layers. This fractal-like behavior is due to the presence of excluded volumes and the finite nature of the system. Experimental observables are considered in detail. An analysis including a general formalism was presented to determine the loss of polarization memory if an excitation is transferred to a random distribution within the given geometrical constraints. The anisotropy decay, which is manifested in a transient grating or fluorescence depolarization experiment, is a direct observable for $G^s(t)$ in DD transfer.

Figure 10 illustrates the nature of the theoretical results. In these calculations the orientation of the molecular transition dipoles is isotropic, i.e., the dipoles can point in any direction in three dimensions. Calculations are for one, two, and three dimensions. The

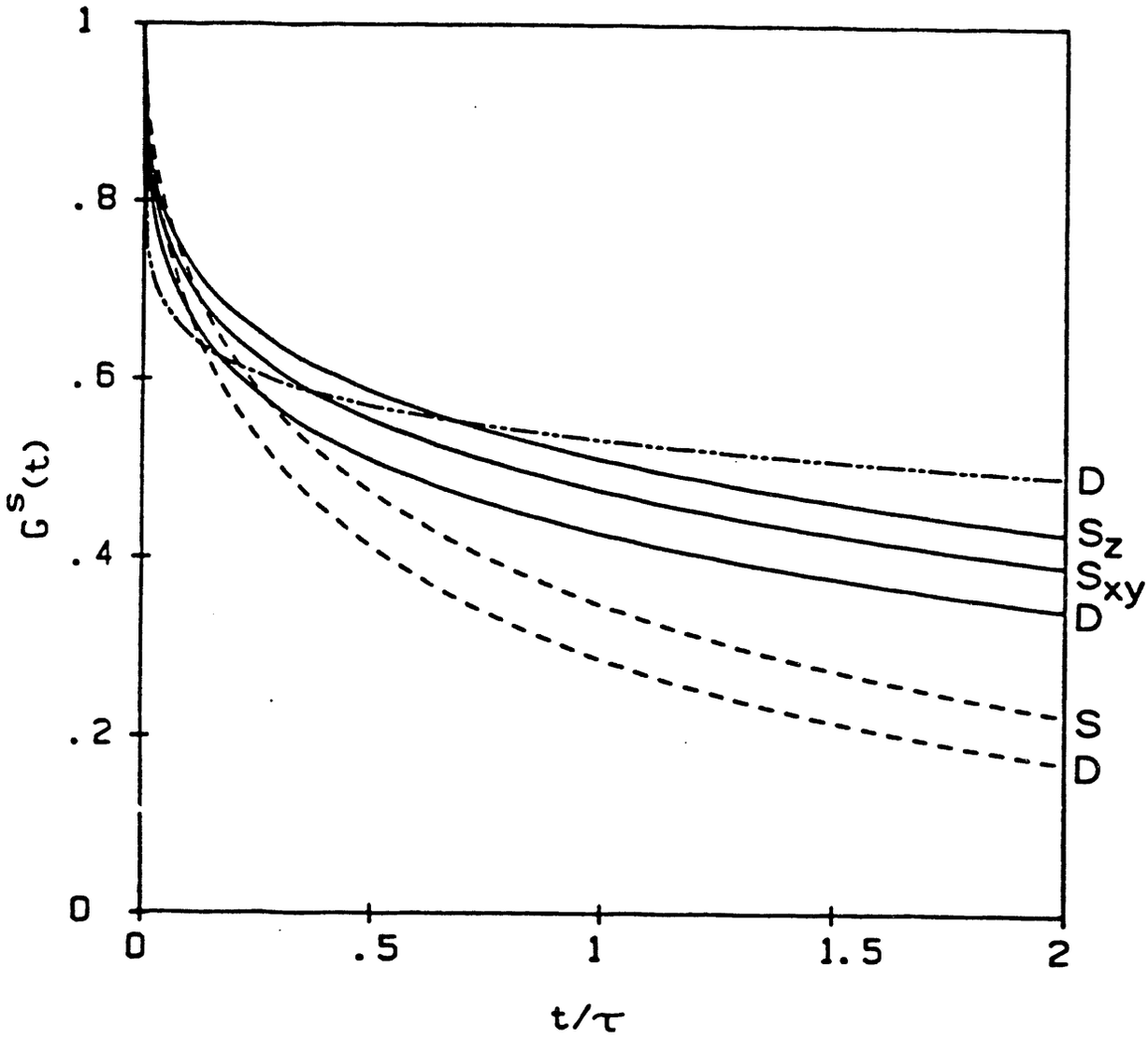

Decay of $G^s(t)$ for infinite systems of different spatial dimension in the DD transfer situation. The lifetime decay $e^{-t/\tau}$ is not included.

Orientation: isotropic

Concentration c = 1

(-·-·-·-) One dimensional

(———) Two dimensional

(- - - -) Three dimensional

D: dynamic limit

S: static limit

S_z: static limit, excitation polarization normal to the plane

S_{xy}: static limit, excitation polarization in the plane.

Figure 10

static limit corresponds to dipole reorientation being very slow relative to the excitation transfer rate. In the dynamic limit, the dipole reorientation is very fast compared to the transfer rate. It is clearly seen that as the spatial dimension becomes lower, the decay is faster at short times and slower at long times. Also in the static isotropic two-dimensional case, the polarization of the excitation field actually influences the rate of energy transport. It is also found that the rate of transport in a monolayer is strongly influenced by confining the dipole direction to be in the plane of the monolayer.

In figure 11 the decay of $G^s(t)$ is shown for a monolayer, and stacks of two up to an infinite number of equally spaced layers for donor-donor transfer in the static limit for isotroic dipole orientation. In this figure the ratio, V, of the Förster radius, R_0, to the interlayer spacing, d, is one. The two-dimensional monolayer reduced chromophore concentration $C_2 = 1$. In the case shown, the infinite layer calculation is almost identical to an isotropic three-dimensional system with concentration, $C_3 = 4/3$. For other concentrations and ratios V, the infinite stack does not behave as a three-dimensional isotropic system.

To investigate excitation transport in layered systems, two types of experimental systems will be studied initially, i.e., aligned multibilayers and vesicles. Multibilayers can be formed from many types of molecules which have liquid crystalline phases. We will initially use phospholipid multibilayers, which are important models for biological membranes. By varying the lipid chain length, different spacings in a bilayer can be achieved. By varying the water content of the multilayered system, the separation from one bilayer to another can be varied.

Two types of chromophores will be studied. The theoretical

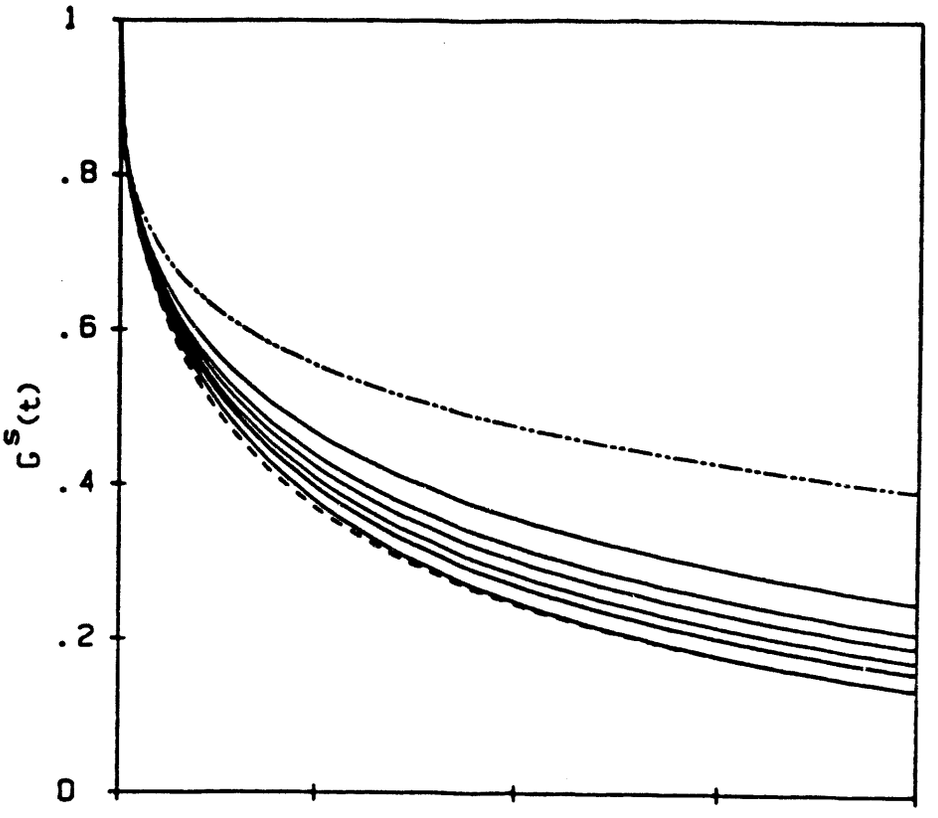

Decay of $G^s(t)$ in mono, bi, and multilayers for DD transfer in the static limit. Lifetime decay $e^{-t/\tau}$ is not included.

Surface concentration: $c_2 = 1$.

Orientation: isotropic

Excitation polarization: parallel to the layers

(—·—·—) Monolayer

(– – – –) Random distribution of the same number of molecules in three dimensions

$R_0/d = 1$

(———) Multilayer, containing, from top to bottom, 2, 3, 4, 6, 10, ∞ equally spaced layers.

(– – – –) Equivalent volume concentration $c_3 = 4/3$

Figure 11

calculations predict well defined differences in systems which have chromophores with transition dipoles constrained to lay in the plane of the layers and with chromophores which can assume isotropic orientations. By using ionic dye head groups with hydrocarbon tails, the chromophores will be located at the surfaces of the layers. In dipalmitoylphosphatidylcholine multibilayers, octadecyl rhodamine B (ODRB) has relatively free rotation of the head group relative to the hydrocarbon tail. ODRB will give a situation in which the dipole orientation is essentially isotropic. 1,1′-dioctadecyl-3,3,3′,3′-tetramethylindodicarbocyanine iodide or the perchlorate have double chains connected to the chromophore head group. The transition dipole lays in the plane at the surfaces of the layers. The double chain prevents the rotation of the dipole out of the layer plane. These dyes are excellent models for the anisotropic (in plane) orientation case.

Because these dyes have relatively short lifetimes (3 nsec) conventional detection of the fluorescence depolarization does not have adequate time response. Polarization grating experiments or fluorescence mixing experiments, as described in Section II, provide the necessary time resolution. The polarization grating experiments will be preferable as they provide better signal to noise ratios and simplify the data analysis in this type of experiment by providing the polarization anisotropy directly. In fluorescence experiments it is necessary to obtain the anisotropy from the parallel and perpendicular components of the fluorescence (see Section III).

The same dye molecules, experimental techniques and theory can be used to study excitation transport in large vesicle (liposome) systems. These vesicles have radii of curvation which are very large compared to the Förster radius, R_0. In this situation, excitation transport is effectively

occurring in bilayer, or multibilayer systems. By carefully controlling the extent of sonication of a phospholipid-water mixture, either single bilayer, or multibilayers can be obtained [32]. The dyes discussed above will go into the lipid phase of the vesicles with the chromophore head groups at the water interfaces. Our earlier work on dye molecules on the surfaces of micelles showed that the micelles permitted much higher local dye concentrations to be achieved, before the onset of excited state quenching by aggregate formation, than could be achieved in normal solutions [11]. These types of systems, which self assemble, are very interesting model systems for the study of excitation transport, and could also be useful in practical solar energy conversion schemes.

V. Photoinduced Electron Transfer and Back Transfer

As discussed in the introduction, the problem of electron transfer into a randomly distributed ensemble of acceptors following optical excitation of a donor was treated by Inokuti and Hiriyama (IH) [22]. Their results can provide an accurate discription of the dynamics of electron transfer monitored by either time resolved or steady state fluorescence quenching [23,24]. The problem involves calculating the dynamics for N acceptors in a volume, V, in a fixed configuration. All the random configurations of acceptors about the donor are then average over, and N and V are increased to infinity keeping their ratio (the concentration of acceptors) constant (the thermodynamic limit).

Once the electron is transferred, a positive and a negative ion are formed. The dynamics of the back transfer process, i. e., the electron returns from the anion to the cation to give the original ground state neutral molecules, has not been examined in detail either experimentally or theoretically. Experiments have principally focused on chemical reaction

yields which arise from cage escape of the ions prior to the competing back transfer process [21]. This is a very indirect observable which does not lend itself to understanding the detailed time dependence of the back transfer step. Theory has focused on the pairwise energetics which influence the process [33], not the important role of the interplay between the forward process, which establishes the nonrandom spatial distribution from which the back transfer occurs, and the back transfer rates. To experimentally extract detailed information on the parameters which govern back transfer, it is necessary to have an observable which is directly related to the back transfer step and a statical mechanics theory which properly relates the back transfer parameters to the observables.

The complexity of this problem arises from the nonrandom distribution of distances which seperate the ensemble of ion pairs formed in the forward transfer process. At time t = 0 the donors are excited. Forward transfer begins to occur. At early time, the forward transfer will principally occur from donors which happen to have nearby acceptors. Ion pairs will be formed which have positions correlated by the rate parameters which govern the forward process. Because the ion pairs formed at early time are very close together, back transfer is very rapid. As time evolves, forward transfer will produce pairs which are more widely seperated. Back transfer from these pairs will be increasingly slow. Therefore the ensemble distribution of separations of anions and cations is not only nonrandom, but it is also time evolving.

Picosecond transient grating experiments provide an observable which is directly related to the back transfer dynamics. To improve the signal to noise ratio for very low levels of excitation which are necessary to avoid artifacts, we are employing polarization grating methods. These

techniques are described in Section II. The transient grating signal is related to the number of donor excited states and the number of ion pairs. Even in the case that all excited states are quenched by electron transfer, there is still a grating signal which is determined only by the number of ion pairs.

Calculation of the transient grating observable requires knowledge of the ensemble averaged time dependent probabilities of the three states of the system

$\langle \rho_{s_1}(t) \rangle$ -- the averaged probability of finding the originally excited donor in the excited state at time t.

$\langle \rho_{s_0}(t) \rangle$ -- the averaged probability of finding the originally excited donor in the ground state at time t.

$\langle \rho^{+}_{s_0}(t) \rangle$ -- the averaged probability of finding the originally excited donor as an ion at time t.

In solving this problem we are assuming a random and immobile distribution of neutral donors and acceptors in the glass and that the donor concentration is low enough that there are no dnor-donor interactions. At t = 0 the initial conditions are $\langle \rho_{s_1}(0) \rangle = 1$, $\langle \rho^{+}_{s_0}(0) \rangle = 0$, $\langle \rho_{s_0}(0) \rangle = 0$.

Following photoexcitation of the donor, there are three significant kinetic processes.

1) Unimolecular excited state decay. The rate constant, $k = 1/\tau_0$ is independenet of acceptor configuration.

2) Donor to acceptor electron transfer. For a single acceptor, i, the rate constant is $k_{F_i} = 1/\tau_0 \, e^{\gamma} \, e^{-R_i/A_F}$, $\gamma = R_0/A_F$, where R_i is the donor-acceptor separation.

3) Reduced acceptor to oxidized donor electron transfer (back transfer). Once formed, the ion pair reverts to the neutral ground state with a rate constant $k_{B_i} = k_R e^{-R_i/A_B}$.

For a single donor surrounded by a fixed configuration of N acceptors

the rate equations for this system are

$$(14) \qquad \dot{\rho}_{s_1} = -\left(k + \sum_{i=1}^{N} k_{F_i}\right)\rho_{s_1}$$

$$(15) \qquad \dot{\rho}_{s_0} = k\rho_{s_1} + \sum_{i=1}^{N} k_{B_i}\rho^{+}_{s_0 i}$$

$$(16) \qquad \dot{\rho}^{+}_{s_i} = k_{Fi}\rho_{s_1} - k_{B_i}\rho^{+}_{s_0 i}\}$$ N separate equations, one for each acceptor

ρ is the number density of the particular species.

This system of equations can be solved analytically for any value of N in a fixed configuration. Calculation of the probabilities requires an average over the distribution of configurations present in the sample. This average can be analytically performed only for ρ_{s_1}. Inokuti and Hirayama [22] have shown that for a random distribution of donors and acceptors

$$(17) \qquad \langle\rho_{s_1}(t)\rangle = \exp\left[- t/\tau_0 - \frac{C}{\gamma^3 C_0}\, g\left(\frac{e^{\gamma t}}{\tau_0}\right)\right]$$

with $\gamma = R_0/A_F$, $C/C_0 = NR_0^3/R_v^3$ where R_v is the radius of the finite volume containing the N acceptors and

$$(18) \qquad g(z) = 6z \sum_{m=0}^{\infty} \frac{(-z)^m}{m!(m+1)^4}$$

for all $z > 0$.

The other averages, $\langle\rho_{s_0}(t)\rangle$ and $\langle\rho^{+}_{s_0}(t)\rangle$, cannot be obtained analytically for an infinite number of acceptors. However, these averages can be obtained analytically for any finite number (N) of acceptors. Therefore we numerically calculate these values using first one acceptor,

then two acceptors, and so on. This represents a hierarchy of approximations which rapidly converge.

These results give all the information needed to calculate the transient grating signal, S(t).

$$(19) \qquad S(t) = A[\langle \rho^{+}_{s_0}(t)\rangle + \langle \rho_{s_1}(t)\rangle]^2$$

The theory has seven parameters. The fluorescence lifetime, τ_0, and the forward transfer parameters, R_0 and A_F, can be determined from fluorescence experiments using the IH theory. The concentrations of donors and acceptors can be measured spectroscopically. This leaves only the two back transfer parameters, k_R and A_B, which are determined by best fit to the experimental data. The signal S(t) has two contributions. $\langle \rho_{s_1}(t)\rangle$ is given by the IH theory from the fluorescence experiments. The theoretical derivation of $\langle \rho^{+}_{s_0}(t)\rangle$, while straightforward, is too lengthy to present in detail here. The time dependent ion concentration $\langle \rho^{+}_{s_0}(t)\rangle$ can be obtained experimentally, and using the theory, the back transfer parameters can be determined.

Figure 12 displays calculated transient grating decays obtained using the theory briefly outlined above. Curve A is for zero acceptor concentration, i. e., it is the lifetime decay. The lifetime and forward parameters are those measured for the system rubrene (donor) and duroquinone (acceptor). For these sample calculations, the forward and back transfer parameters were set equal to each other. The parameters and concentrations are listed in the figure caption. As the acceptor concentration is increased, the decays become increasingly rapid at short time. Notice that at long time the decays with acceptors become slower than the excited state lifetime decay. These curves are highly nonexponential and are very sensitive to the concentration and the choice

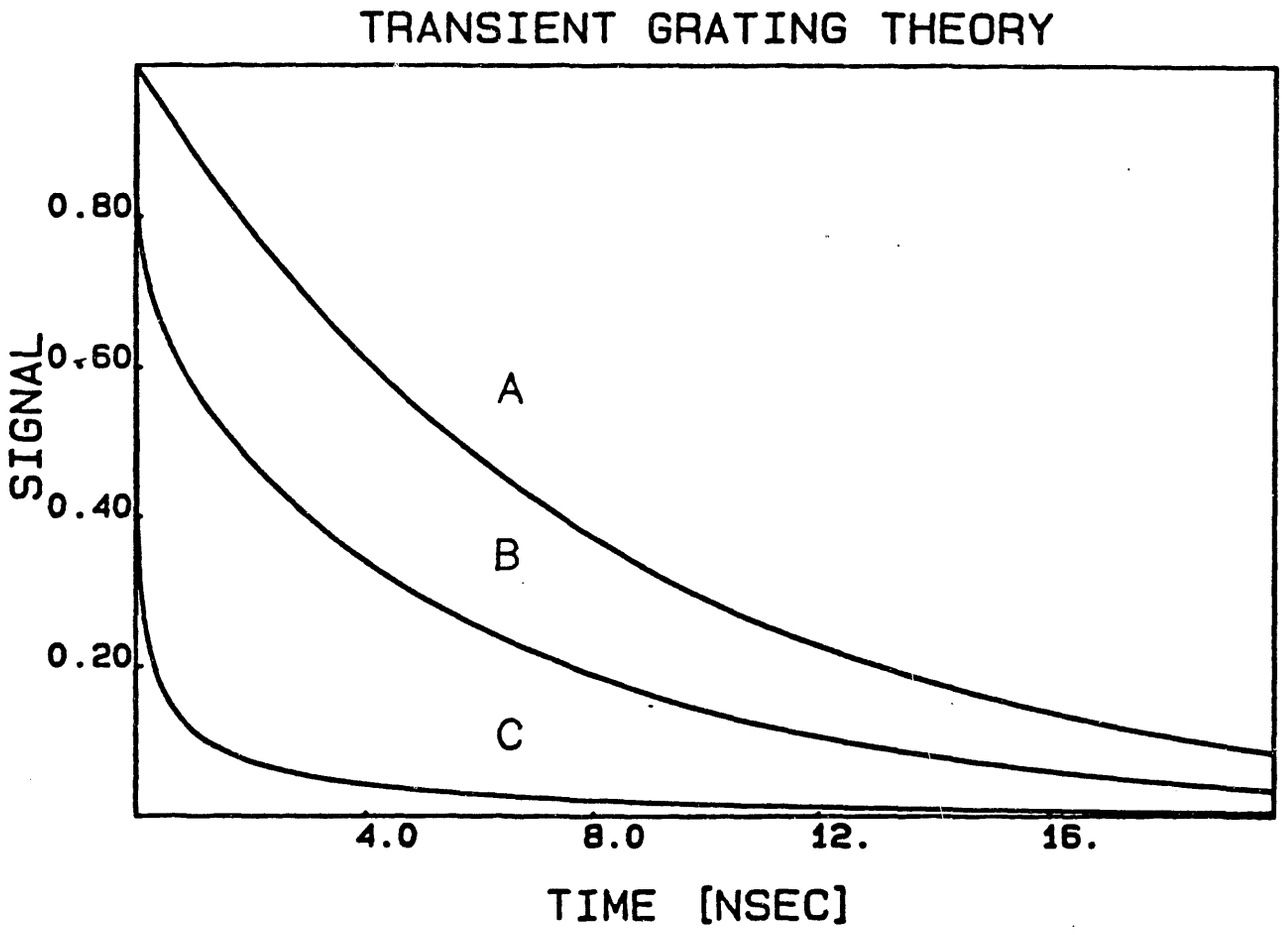

Calculated transient grating decay curves. The donor is rubrene, and the acceptor is duroquinone. The forward electron transfer parameters are those measured for the rubrene-duroquinone system. Lifetime=16.2 nsec; a_f=0.65 Å; R_o=10.5 Å. For this calculation the back transfer parameters were set equal to the forward parameters. a_b=0.65 Å and k_r=6.5 x 10^5 $nsec^{-1}$. The acceptor concentrations are A) 0.0 M; B) 0.089 M; C) 0.367 M.

Figure 12

of back transfer parameters. Figure 13 shows transient grating data taken on the rubrene-duroquinone system. The spike at time t = 0 is a coherence artifact. Curve A has zero acceptor concentration, i. e., it is the life time decay. The other curves have the same concentrations used to calculate curves in Fig. 12.

We are now in a position to perform detailed studies of the back transfer process. To accurately compare theory to experiment, it is necessary to convolve the theoretical curves with the instrument response function. At the time of this writing, the convolution procedure is being implimented. The detailed comparison of theory and experiment will provide the first direct examination of the time dependence of the back transfer process. We will examine a variety of acceptors such as duroquinone, dimethyl benzoquinone, benzoquinone, chloronil, etc. We can also examine a variety of donors. Of particular interest will be studying the effects of the medium for the identical donor-acceptor system. Currently we are using a sucrose octa-acetate glass, which is polar. Other glasses, such as trinaphthylbenzene, which are nonpolar will also be studied. The ability of the medium to reorganize will not necessarily influence the forward and back transfer processes in the same manner. Temperature is another important parameter to vary to understand the reorganization of the medium and its influence on the forward and back transfer processes. It should be pointed out that these experiments will examine the forward process as well as the back transfer process in great detail.

The theory and experiments described above will greatly increase our understanding of the relationship between the forward and back transfer processes in systems in which diffusion of the ions is not possible. Once the theoretical treatment of the forward and back transfer process has been

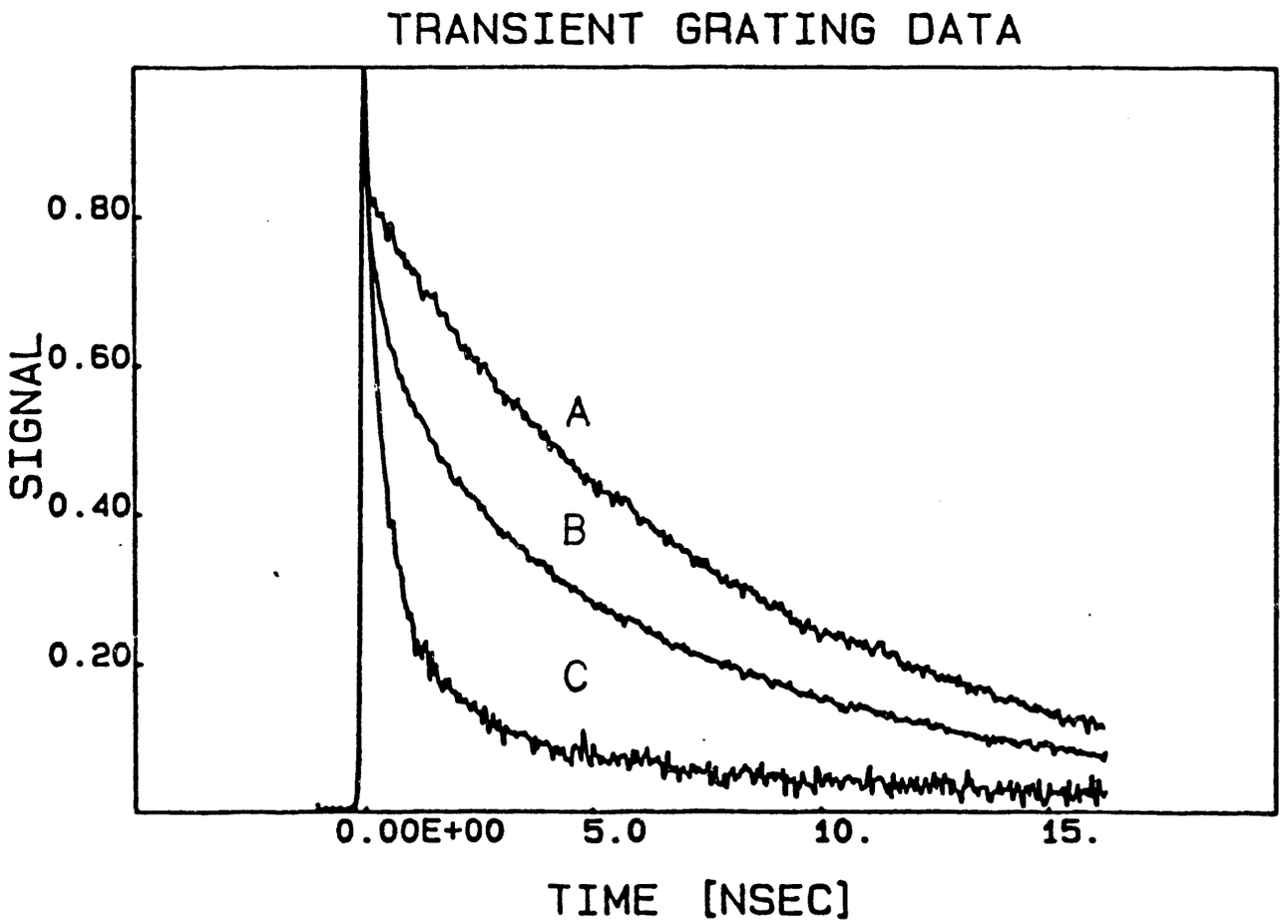

Transient grating data taken on the rubrene-duroquinone system. The decay reflects both the forward and back transfer processes. The duroquinone (acceptor) concentrations are A) 0.0 M; B) 0.089 M; C) 0.367 M. The spike at very short time is a coherence artifact. The forward electron transfer parameters are measured with time resolved fluorescence experiments. This permits the electron back transfer parameters to be extracted from the transient grating data.

Figure 13

varified, we will also examine donor-acceptor systems in solutions of decreasing viscosity. This will begin to provide insights into the competition between back transfer and diffusional seperation of the ions. The theory described above is the starting point for a theory which will include diffusion.

References

1. Th. Förster, Ann. Phys. Leipzig 2, 55 (1948).
   Th. Förster, Z. Naturforsch. Teil A 4, 321 (1949).
2. C. R. Gochanour, H. C. Andersen, M. D. Fayer, J. Chem. Phys. 70, 4254 (1979).
3. S. W. Haan and R. Zwanzig, J. Chem. Phys. 68, 1879 (1978).
4. C. R. Gochanour and M. D. Fayer, J. Phys. Chem. 85, 1989 (1981).
5. R. F. Loring, H. C. Andersen, and M. D. Fayer, J. Chem. Phys. 76, 2015 (1982); 77, 1079(E) (1982).
6. R. J. D. Miller, M. Pierre, and M. D. Fayer, J. Chem. Phys. 78, 5138 (1983); D. P. Millar, R. J. Robbins, and A. H. Zewail, J. Chem. Phys. 75, 3649 (1981).
7. R. F. Loring, H. C. Andersen, and M. D. Fayer, Chem. Phys. 85, 149 (1984).
8. R. Parson, Chem. Phys. Lett. 99, 213 (1983).
9. G. H. Fredrickson, H. C. Andersen, and C. W. Frank, Macromolecules 16 1456 (1983); 17, 1496 (1984); J. Chem. Phys. 79, 3572 (1983).
10. M. D. Ediger and M. D. Fayer, J. Chem. Phys. 78, 2518 (1983).
11. M.D. Ediger, R. P. Domingue, and M. D. Fayer, J. Chem. Phys. 80, 1246 (1984).
12. M. D. Ediger and M. D. Fayer, Macromolecules 16, 1839 (1983).
13. G. H. Fredrickson, H. C. Andersen, and C. W. Frank, Macromolecules 79, 3572 (1983); 17, 54 (1984).
14. M. D. Ediger, R. P. Domingue, K. A. Peterson, and M. D. Fayer, Macromolecules 18, 1182 (1985).
15. K. A. Peterson and M. D. Fayer, J. Chem. Phys. 85, 4702 (1986).

16. K. A. Peterson, M. B. Zimmt, S. Linse, R. P. Domingue, and M. D. Fayer, Macromolecules, accepted (1986).

17. R. F. Loring and M. D. Fayer, Chem. Phys. 70, 139 (1982).

18. P. Anfinrud, R. L. Crackel, and W. S. Struve, J. Phys. Chem. 88, 5873 (1984); P. A. Anfinrud, D. E. Hart, J. F. Hedstrom, and W. S. Struve, J. Phys. Chem. 90, in press (1986).

19. D. L. Huber, Phys. Rev. B 20, 2307 (1979); 20, 5333 (1979).

20. J. Baumann and M. D. Fayer, J. Chem. Phys. 85, 4087 (1986).

21. Noborv Mataya, Yu Kanda, and Tadashi Okada, J. Phys. Chem. 90. 3880 (1986); Yoshinori Hirata and Noborv Mataya, 89, 2439 (1985).

22. M. Inokuti and F. Hirayama, J. Chem. Phys. 43, 1978 (1965).

23. S. Strach, G. McLendon, M. McGuire, and T. Grover, J. Phys. Chem. 87, 3579 (1983); A. Namiki, N. Nakashima, and K. Yoshihara, J. Chem. Phys. 71, 925 (1979); R. K. Huddleston and J. R. Miller, J. Phys. Chem. 86, 200 (1982).

24. R. P. Domingue and M. D. Fayer, J. Chem. Phys. 83, 2242 (1985).

25. D. R. Lutz, K. A. Nelson, C. R. Gochanour, and M. D. Fayer, Chem. Phys. 58, 325 (1981); M. D. Fayer, Ann. Rev. Phys. Chem. 33, 63 (1982); Todd S. Rose, Roberto Righini, and M. D. Fayer, Chem. Phys. Lett. 106, 13 (1984); Keith A. Nelson, R. J. Dwayne Miller, D. R. Lutz, and M. D. Fayer, J. Appl. Phys. 53, 1144 (1982).

26. A. von Jena and H. E. Lessing, Opt. Quantum Electron. 11, 419 (1979); G. Eyring and M. D. Fayer, J. Chem. Phys. 81, 4314 (1984).

27. H. Yamakawa, "Modern Theory of Polymer Solutions," Harper and Row, New York, 1971, Chapt. 2.

28. P. J. Flory, "Statistical Mechanics of Chain Molecules"; Interscience Publishers:New York, 1969.

29. R. G. Kirste, W. A. Kruse, and K. Ibel, Polymer 16m 120 (1975).

30. H. Hayashi, P. J. Flory, and G. D. Wignall, Macromolecules 16, 1328 (1983).

31. J. Brandrup, E. H. Immergut, editors "Polymer Handbook," JJohn Wiley and Sons:New York, 1975. Section IV.

32. F. Szoka and D. Papahadjopoulos in Liposomes: from Physical Structure to Therapeutic Applications, Ed. C. G. Knight, Elsevier/North Holland, Amsterdam, 1981 (p. 51).

33. Toshiaki Kakitani and Noborv Mataga, J. Phys. Chem. 90, 993 (1986); 89, 4752 (1983).

Michael D. Fayer

Born: September 12, 1947 in Los Angeles, California

Marital Status: Married, one child

Education:
Public schools in Los Angeles, California, 1953-1965
University of California at Berkeley, 1965-1969
B.S. 1969
Undergraduate National Science Foundation Fellow;
Phi Beta Kappa
University of California at Berkeley, 1969-1974
Ph.D. 1974

Academic Positions:
Assistant Professor of Chemistry, Stanford University
September 1974 - August 1980
Associate Professor of Chemistry, Stanford University
September 1980 - August 1984
Professor of Chemistry, Stanford University
September 1984 on

Affiliations and Honors:
American Chemical Society
American Physical Society
Sigma Xi
Guggenheim Foundation Fellow
Fellow of the American Physical Society
Alfred P. Sloan Fellow
Camille and Henry Dreyfus Foundation Fellow
Arthur D. Little Lecturer, Massachusetts Institute of
Technology, Chemistry Department, 1980
Professor of Physics, University of Grenoble,
Grenoble, France, 1982
Advisory Editor, Journal of Luminescence
Advisory Editor, Chemical Physics Letters
Advisory Editor, Chemical Physics
Chairman; Fourth International Conference of Dynamical
Processes; Stanford, 1983

Principal Research Interests:
Principal research interests are in areas involving excited state dynamics of molecules in condensed phases. The development and use of nonlinear optical techniques such as picosecond optical coherence experiments combined with more conventional optical methods and theory to investigate electronic excited state energy transport, excited state-excited state and excited state-environment interactions, and radiationless processes. Optical generation of acoustic waves and their application to the study of acoustic properties of materials, in particular membrane like systems. Study of polymers and polymer blends using picosecond optical methods. Nonphotochemical hole burning using ultrahigh resolution dye lasers. Statistical mechanics of energy transport in disordered systems. Electron transport in molecular systems.

Publications of Michael D. Fayer

1. "Transition Metal Nuclear Quadrupole Resonance IV. Mangenese--55 Nuclear Quadrupole Resonance in pi-Pyrrolenylmanganese Tricarbonyl and pi-Cyclopentadienylmanganese Tricarbonyl and pi-Pyrrolenyl-Metal Bonds." M. D. Fayer and C. B. Harris, Inorganic Chemistry 8, 2792 (1969).

2. "Optically Detected Nuclear Quadrupole Resonance and Transferred Hyperfine Coupling via Guest-Host Interactions," M. D. Fayer, C. B. Harris, and D. A. Yuen, J. Chem. Phys. 53, 4719 (1970).

3. "Trapping of Coherent Triplet Excitons in Molecular Crystals." M. D. Fayer and C. B. Harris, 1972 Pacific Conference on Chemistry and Spectroscopy, San Francisco, California, October 1972.

4. "Coherent Energy Migration in Solids I. Band-Trap Equilibria at Boltzmann and non-Boltzmann Temperatures." M. D. Fayer and C. B. Harris, Physical Review B 9, 748 (1974).

5. "Coherent Energy Migration in Solids II. Spin Resonance Absorption in Coherent Wave Packet States and the Effects of Phonon-Exciton Scattering." C. B. Harris and M. D. Fayer, Physical Review B 10, 1784 (1974).

6. "The Decay of Localized States Into Delocalized Band States I. Theory and Preliminary Experimental Investigations Using Optically Detected Electron Spin Coherence." M. D. Fayer and C. B. Harris, Chem. Phys. Lett. 25, 149 (1974).

7. "Direct Measurement of the Quantum Yield for the Creation of Mobile Excitons From Localized States Using Optically Detected Electron Spin Coherence." H. C. Brenner, J. C. Brock, M. D. Fayer, and C. B. Harris, Chem. Phys. Lett. 33, 471 (1975).

8. "Coherence in Multilevel Systems. II. Description of a Multilevel System as Two Levels in Contact with a Population Reservoir," W. G. Breiland, M. D. Fayer, and C. B. Harris, Phys. Rev. A13, 383 (1976).

9. "Experimental Determination of the Triplet Exciton Intermolecular Interaction Matrix Element and the Exciton-Phonon Scattering Rate in Molecular Crystals," D. D. Dlott and M. D. Fayer, Chem. Phys. Lett. 41, 305 (1976).

10. "On the Temperature Dependence of Excited Triplet State Spin Sublevel Populations of Shallow Traps in Molecular Crystals," M. D. Fayer and C. R. Gochanour, J. Chem. Phys. 65, 2472 (1976).

11. "Coherent One-Dimensional Exciton Transport and Impurity Scattering," D. D. Dlott, M. D. Fayer, and R. D. Wieting, J. Chem. Phys. 61, 3808 (1977).

12. "Triplet Exciton Spectral Line Shapes in Molecular Crystals: 1,2,4,5-Tetrachlorobenzene," D. M. Burland, D. E. Cooper, M. D. Fayer, and C. R. Gochanour, Chem. Phys. Lett. 52, 279 (1977).

13. "Spin-Orbit Coupling in Exciton Bands of Molecular Crystals," D. E. Cooper and M. D. Fayer, J. Chem. Phys. 68, 229 (1978).

14. "The Effects of Impurity Scattering and Transport Topology on Trapping in Quasi-One-Dimensional Transport Systems: Application to Frenkel Excitons in Molecular Crystals," R. D. Wieting, M. D. Fayer, and D. D. Dlott, J. Chem. Phys. 69, 1996 (1978).

15. "Spin Lattice Relaxation in Triplet States of Isolated Molecules and Pure Crystals in Zero Field," D. R. Lutz, K. A. Nelson, R. W. Olson, and M. D. Fayer, J. Chem. Phys. 69, 4319 (1978).

16. "Effects of Impurity Scattering and Transport Topology on Exciton Migration and Trapping: An Experimental Study of Quasi-One-Dimensional Molecular Crystals," D. D. Dlott, M. D. Fayer, and R. D. Wieting, J. Chem. Phys. 69, 2752 (1978).

17. "Dynamics of Energy Transport in Molecular Crystals: The Picosecond Transient-Grating Method," J. R. Salcedo, A. E. Siegman, D. D. Dlott, and M. D. Fayer, Phys. Rev. Lett. 41, 131 (1978).

18. "Energy Transport in Molecular Solids: Application of the Picosecond Transient Grating Technique," D. D. Dlott, M. D. Fayer, J. Salcedo, and A. E. Siegman in Picosecond Phenomena, C. V. Shank, E. P. Ippen, and S. L. Shapiro, Eds., Springer-Verlag, Berlin Heidelberg New York (1978) p. 240.

19. "Electronic Excited State Transport in Solutions," C. R. Gochanour, Hans C. Andersen, and M. D. Fayer, J. Chem. Phys. 70, 4254 (1979).

20. "Picosecond Time Scale Optical Coherence Experiments in Mixed Molecular Crystals: Pentacene in Naphthalene," D. E. Cooper, R. W. Olson, R. D. Wieting, and M. D. Fayer, Chem. Phys. Lett. 67, 41 (1979).

21. "Excited State Dynamics in Pure Molecular Crystals: Perylene and the Excimer Problem," K. A. Nelson, D. D. Dlott, and M. D. Fayer, Chem. Phys. Lett. 64, 88 (1979).

22. "Excited State Transport in Molecular Systems: Spatially Resolved Picosecond Spectroscopy," M. D. Fayer, Bul. Am. Phys. Soc. 24, 326 (1979).

23. "Exciton Scattering and the Dephasing of ESR and Optical Absorption Lines: The 1,2,4,5-Tetrachlorobenzene Triplet Exciton Problem," R. D. Wieting and M. D. Fayer, J. Chem. Phys. 73, 744 (1980).

24. "Laser Induced Phonons: A Probe of Intermolecular Interactions in Molecular Solids," Keith A. Nelson and M. D. Fayer, J. Chem. Phys. 72, 5202 (1980).

25. "Intermolecular Interaction Dynamics and Optical Dephasing: Picosecond Photon Echo Measurements in Mixed Molecular Crystals," D. E. Cooper, R. W. Olson, and M. D. Fayer, J. Chem. Phys. 74, 2332 (1980).

26. "Site-Dependent Vibronic Line Widths and Relaxation in the Mixed Molecular Crystal Pentacene in p-Terphenyl," R. W. Olson and M. D. Fayer, J. Phys. Chem. 84, 2001 (1980).

27. "Concentration-Dependent Optical Dephasing in Mixed Molecular Crystals: Picosecond Photon Echo Measurements," R. W. Olson and M. D. Fayer, Proceedings of the Ninth Molecular Crystals Symposium, Deutsche Forschungsgemeinschaft Max-Planck Gesellschaft, 1980.

28. "Exciton Coherence," in "Spectroscopy and Excitation Dynamics of Condensed Molecular Systems," M. D. Fayer, Ed. V. M. Agranovich and R. M. Hochstrasser, North Holland (1983).

29. "Delocalized Electronic Excitations of Pentacene Dimers in a p-Terphenyl Host: Picosecond Photon Echo Experiments," R. W. Olson, F. G. Patterson, H. W. H. Lee, and M. D. Fayer, Chem. Phys. Lett. 79, 403 (1981).

*30. "Electronic Excited State Energy Transfer, Trapping by Dimers and Fluorescence Quenching in Concentrated Dye Solutions: Picosecond Transient Grating Experiments," D. R. Lutz, Keith A. Nelson, C. R. Gochanour, and M. D. Fayer, Chemical Physics 58, 325 (1981).

*31. "Electronic Excited State Transport in Random Systems: Time Resolved Fluorescence Depolarization Measurements," C. R. Gochanour and M. D. Fayer, J. Phys. Chem. 85, 1989 (1981).

32. "Laser Induced Phonon Spectroscopy: Optical Generation of Ultrasonic Waves and Investigation of Electronic Excited State Interactions in Solids," Keith A. Nelson, D. R. Lutz, Larry Madison, and M. D. Fayer, Phys. Rev. B 24, 3261 (1981).

33. "Correlation Function Analysis of Coherent Optical Transients and Fluorescence from a Quasi Two Level System," J. L. Skinner, Hans C. Andersen, and M. D. Fayer, Phys. Rev. A 24, 1994 (1981).

34. "Luminescent Solar Concentrators and the Reabsorption Problem," R. W. Olson, Roger F. Loring, and M. D. Fayer, Applied Optics 20, 2934 (1981).

35. "Theory of Photon Echoes from a Pair of Coupled Two Level Systems: Impurity Dimers and Energy Transfer in Molecular Crystals," J. L. Skinner, Hans C. Andersen, and M. D. Fayer, J. Chem. Phys. 75, 3195 (1981).

36. "Nonphotochemical Hole Burning in the Mixed Molecular Crystal Pentacene in Benzoic Acid," F. G. Patterson, H. W. H. Lee, R. W. Olson, and M. D. Fayer, Chem. Phys. Lett. 84, 59 (1981).

37. "Optical Density Effects in Photon Echo Experiments," R. W. Olson, H. W. H. Lee, F. G. Patterson, and M. D. Fayer, J. Chem. Phys. 76, 31 (1982).

38. "Electronic Excited State Transport and Trapping in Solution," Roger F. Loring, Hans C. Andersen, and M. D. Fayer, J. Chem. Phys. 76, 2015 (1982).

39. "Optical Generation of Tunable Ultrasonic Waves," Keith A. Nelson, R. J. Dwayne Miller, D. R. Lutz, and M. D. Fayer, J. Appl. Phys. 53, 1144 (1982).

40. "Electronic Excited State Transport and Trapping in One and Two Dimensional Disordered Systems," Roger F. Loring and M. D. Fayer, Chem. Phys. 70, 139 (1982).

41. "On the Refractive Index Correction in Luminescence Spectroscopy," M. D. Ediger, R. S. Moog, S. G. Boxer, and M. D. Fayer, Chem. Phys. Lett. 88, 123 (1982).

42. "Dynamics of Molecules in Condensed Phases: Picosecond Holographic Grating Experiments," M. D. Fayer, Ann. Rev. Phys. Chem. 33, 63 (1982).

43. "Picosecond Transient Grating Generation of Tunable Ultrasonic Waves," Keith A. Nelson, R. J. Dwayne Miller, D. R. Lutz, and M. D. Fayer, in "Proceedings of the SPIE Conference on Picosecond Lasers/Applications," Vol. 322, Los Angeles (1982).

*44. "Electronic Excited State Transport and Trapping in Disordered Systems," M. D. Fayer, "Proceedings of the 10th Molecular Crystals Symposium" Quebec, Canada (1982).

45. "Nonphotochemical Hole Burning and Antihole Production in the Mixed Molecular Crystal Pentacene in Benzoic Acid," R. W. Olson, F. G. Patterson, H. W. H. Lee, M. D. Fayer, R. M. Macfarlane, and R. M. Shelby, J. Chem. Phys. 77, 2283 (1982).

46. "Viscosity Dependence of the Rotational Reorientation of Rhodamine B in Mono- and Polyalcohol. Picosecond Transient Grating Experiments," R. S. Moog, M. D. Ediger, S. G. Boxer and M. D. Fayer, J. Phys. Chem. 86, 4694 (1982).

47. "Laser Induced Excited State and Ultrasonic Wave Gratings: Amplitude and Phase Grating Contributions to Diffraction," Keith A. Nelson, R. Casalegno, R. J. Dwayne Miller, and M. D. Fayer, J. Chem. Phys. 77, 1144 (1982).

48. "Laser-Induced Ultrasonics: A Dynamic Holographic Approach to the Measurement of Weak Absorptions, Opto-elastic Constants and Acoustic Attenuation," R. J. Dwayne Miller, R. Casalegno, Keith A. Nelson, and M. D. Fayer, Chem. Phys. 72, 371 (1982).

49. "Temperature Dependent Dephasing of Delocalized Dimer States of Pentacene in p-Terphenyl: Picosecond Photon Echo Experiments," H. W. H. Lee, F. G. Patterson, R. W. Olson, D. A. Wiersma, and M. D. Fayer, Chem. Phys. Lett. 90, 172 (1982).

*50. "Electronic Excited State Transport and Trapping in Disordered Systems: Picosecond Fluorescence Mixing, Transient Grating, and Probe Pulse Experiments," R. J. Dwayne Miller, Marc Pierre, and M. D. Fayer, J. Chem. Phys. 78, 5138 (1983).

*51. "Electronic Excited State Transport Among Molecules Distributed Randomly in a Finite Volume," M. D. Ediger and M. D. Fayer, J. Chem. Phys. 78, 2518 (1983).

52. "Picosecond Holographic Grating Experiments on Molecular Condensed Phases," M. D. Fayer in Picosecond Phenomena III, eds., K. B. Eisenthal, R. M. Hochstrasser, W. Kaiser, and A. Laubereau, Springer-Verlag, Berlin Heidelberg New York, p. 82 (1982).

*53. "A New Approach to Probing Polymer and Polymer Blend Structure Using Electronic Excitation Transport," M. D. Ediger and M. D. Fayer, Macromolecules 16, 1829 (1983).

54. "Excitation Transport on Substitutionally Disordered Lattices," Roger F. Loring, Hans C. Andersen and M. D. Fayer, Phys. Rev. Lett. 50, 1324 (1983).

55. "Holographic Generation of Bubble Gratings at Liquid-Glass Interfaces and the Dynamics of Bubbles on Surfaces," Gregory Eyring and M. D. Fayer, Chem. Phys. Lett. 98, 428 (1983).

56 "Excitation Transport on Substitutionally Disordered Lattices," R. F. Loring, Hans C. Andersen, and M. D. Fayer, J. Opt. Soc. America, 73, 1388 (1983).

57. "Hopping Transport on a Randomly Substituted Lattice for Long Range and Nearest Neighbor Interactions," Roger F. Loring, Hans C. Andersen, and M. D. Fayer, J. Chem. Phys. 80, 5731 (1984).

58. "Hopping Transport on a Randomly Substituted Lattice in the Presence of Dilute Deep Traps," Roger F. Loring, Hans C. Andersen, and M. D. Fayer, Chem. Phys. 85, 149 (1984).

59. "Laser-Induced Phenomena at Liquid-Glass Interfaces: Particle Deposition and Holographic Bubble Grating Formation," Gregory Eyring and M. D. Fayer, J. Appl. Phys. 55, 4072 (1984).

**60. "Picosecond Studies of Excitation Transport in a Finite Volume: The Clustered Transport System Octadecyl Rhodamine B in Triton X-100 Micelles," M. D. Ediger, R. P. Domingue, and M. D. Fayer, J. Chem. Phys. 80, 1246 (1984).

61. "Intersystem Crossing from Singlet States of Molecular Dimers and Monomers in Mixed Molecular Crystals: Picosecond Stimulated Photon Echo Experiments," F. G. Patterson, H. W. H. Lee, William L. Wilson, and M. D. Fayer, Chem. Phys. 84, 51 (1983).

**62. "Excitation Transport and Trapping in a Synthetic Chlorophyllide Substituted Hemoglobin: Orientation of the Chlorophyll S_1 Transition Diple," Richard S. Moog, Atsuo Kuki, M. D. Fayer, and Steven G. Boxer, Biochemistry 23, 1564 (1984).

63. "A Coherent Photoacoustic Approach to Excited State-Excited State Absorption Spectroscopy: Application to the Investigation of A Near Resonant Contribution to Ultrasonic Diffraction," R. J. Dwayne Miller, Marc Pierre, Todd S. Rose, and M. D. Fayer, J. Phys. Chem. 88, 3021, (1984).

**64. "Electronic Excitation Transport in Disordered Finite Volume Systems," M. D. Ediger and M. D. Fayer, J. Phys. Chem. 88, 6108 (1984).

65. "Picosecond Holographic Generation of Ultrasonic Waves and Application to Spectroscopic and Physical Measurements," M. D. Fayer, Proceedings of The International Conference on Lasers '83; Ed.: R. C. Powell, STS Press, McLean, VA, p. 337 (1984).

**66. "Electronic Excitation Transport in Disordered and Finite Volume Systems," M. D. Fayer, Proceedings of The International Conference on Lasers '83; Ed.: R. C. Powell, STS Press, McLean, VA, p. 694 (1983).

67. "Picosecond Transient Grating Measurements of Singlet Exciton Transport in Anthracene Single Crystals," Todd S. Rose, Roberto Righini, and M. D. Fayer, Chem. Phys. Lett. 106, 13 (1984).

68. "Inhomogeneous Broadening of Electronic Transitions of Chromophores in Crystals and Glasses: Analysis of Hole Burning and Fluorescence Line Narrowing Experiments," H. W. H. Lee, C. A. Walsh, and M. D. Fayer, J. Chem. Phys. 82(9) 3948 (1985).

69. "A Picosecond Holographic Grating Approach to Molecular Dynamics in Oriented Liquid Crystal Films," Gregory Eyring and M. D. Fayer, J. Chem. Phys. 81, 4314 (1984).

70. "A Laser Induced Ultrasonic Probe of the Mechanical Properties of Aligned Lipid Multibilayers," Gregory Eyring and M. D. Fayer, Biophys. J. 47, 37 (1985).

71. "Transient Properties of Triplet Bottleneck Holeburning in an Optically Thick Sample," F. W. Deeg, Larry Madison, and M. D. Fayer, Chem. Phys. 94, 265 (1985).

72. "Optical Dephasing of Molecular Dimers in Mixed Crystals: Picosecond Photon Echo Experiments," F. G. Patterson, William L. Wilson, H. W. H. Lee, and M. D. Fayer, Chem. Phys. Lett. 110, 7 (1984).

73. "Excitation Transport and Dynamics in Solid State Systems," M. D. Fayer, J. Lumin. 31-32, 525 (1984).

74. "Theory of Photon Echoes from Interacting Impurities in Crystals with Inhomogeneously Broadened Absorption Spectra," Roger F. Loring, Hans C. Andersen, and M. D. Fayer, J. Chem. Phys. 81(12), 5395 (1984).

**75. "Determination of the Guest Radius of Gyration in Polymer Blends: Excitation Transport Induced Time Resolved Fluorescence Depolarization," M. D. Ediger, R. P. Domingue, K. A. Peterson, and M. D. Fayer, Macromolecules 18, 1182 (1985).

76. "Probing Gas Phase Dynamics with Picosecond Transient Grating Spectroscopy," Todd S. Rose and M. D. Fayer, Chem. Phys. Lett. 117(1), 12 (1985).

77. "Nonphotochemical Hole Burning and Intersystem Crossing in the Pentacene/Benzoic Acid System: Deuterium Effects," C. A. Walsh and M. D. Fayer, J. Lumin. 34, 37 (1985).

**78. "Electronic Excitation Transport in Disordered Infinite Volume Systems," M. D. Ediger and M. D. Fayer, Int. Rev. Phys. Chem., Vol. 4(3), 207 (1985).

**79. "Electron Transfer Between Molecules Randomly Distributed in a Glass," R. P. Domingue and M. D. Fayer, J. Chem. Phys. 83(5), 2242 (1985).

**80. "Surface Quenching of Optically Generated Carriers in Thin Film Hydrogenated Amorphous Silicon: Picosecond Transient Grating Experiments," Vincent J. Newell, Todd S. Rose, and M. D. Fayer, Phys. Rev. B. 32(12), 8035 (1985).

81. "The Effect of Cholesterol on the Viscoelastic Properties of Dipalmitoylphosphatidyl Choline Multibilayers, as Measured by a Laser Induced Ultrasonic Probe," M. Y. El-Sayed, T. A. Guion, and M. D. Fayer, Biochemistry 25, 4825 (1986).

82. Optical Dephasing of the Electronic Transitions of Delocalized Molecular Dimer States," H. W. H. Lee and M. D. Fayer, J. Chem. Phys. 84, 5463 (1986).

**83. "Excitation Transfer in Disordered Two-Dimensional and Anisotropic Three-Dimensional Systems: Effects of Spatial Geometry on Time-Resolved Observables," J. Baumann and M. D. Fayer, J. Chem. Phys. 85, 4087 (1986).

**84. "The Influence of Orientational Fluctuations on Electron Transfer in Systems of Donor-Acceptor Pairs," R. P. Domingue and M. D. Fayer, J. Phys. Chem., accepted (1986).

**85. "Electronic Excitation Transport on Isolated, Flexible Polymer Chains in Amorphous Solids Randomly Tagged or End Tagged with Chromophores," Kristen A. Peterson and M. D. Fayer, J. Chem. Phys. 85 4702 (1986).

86. "Delocalization of Electronic Excitations in Disordered Molecular Systems," R. J. Gulotty, C. A. Walsh, F. G. Patterson, William L. Wilson, and M. D. Fayer, Chem. Phys. Lett. 125, 507 (1986).

87. "Picosecond Holographic Grating Generation of Ultrasonic Waves," M. D. Fayer, IEEE J. Quantum Electronics, accepted (1986).

**88. "Picosecond Transient Grating Experiments on Hydrogenated Amorphous Silicon: Models for Surface Quenching," Vincent J. Newell and M. D. Fayer, The Second International Conference on Unconventional Photoactive Solids (Plenum Publishing, New York, 1987).

**89. "Quantitative Determination of the Radius of Gyration of Poly(Methyl Methacrylate) in the Amorphous Solid State by Time-Resolved Fluorescence Depolarization Measurements of Excitation Transport," K. A. Peterson, M.B. Zimmt, S. Linse, R. P. Domingue, and M. D. Fayer, Macromolecules, accepted (1986).

90. "Probing Intermolecular Interactions with Picosecond Photon Echo Experiments," C. A. Walsh, M. Berg, L. R. Narasimhan, and M. D. Fayer, Accounts of Chemical Research, submitted (1986).

91. "Picosecond Transient Grating Experiments in Sodium Vapor: Velocity and Polarization Effects," Todd S. Rose, William L. Wilson, G. Wäckerle, and M. D. Fayer, Phys. Rev. Lett., submitted (1986).

92. "Theory of the Phonon Perturbed Photon Echo Experiment: Direct Determination of Electronic Excitation-Phonon Coupling," William L. Wilson, G. Wäckerle, and M. D. Fayer, J. Chem. Phys., submitted (1986).

93. "Ultrafast Dephasing in a Low Temperature Organic Glass," C. A. Walsh, M. Berg, L. R. Narasimhan, Karl A. Littau, and M. D. Fayer, Chem. Phys. Lett., submitted (1986).

94. "A Picosecond Photon Echo Study of a Chromophore in an Organic Glass: Temperature Dependence and Comparison to Non-Photochemical Hole Burning," C. A. Walsh, M. Berg, L. R. Narasimhan, and M. D. Fayer, J. Chem. Phys., accepted (1986).

95. "Optical Dephasing of Chromophores in an Organic Glass: Picosecond Photon Echo and Hole Burning Experiments," C. A. Walsh, M. Berg, L. R. Narasimhan, and M. D. Fayer, Chem. Phys. Lett. 130, 6 (1986).

** 96. "Determination of the Ensemble Average Conformation of Isolated Polymer Coils in Solid Blends Using Electronic Excitation Transport: Theory and Experiment," K. A. Peterson, M. B. Zimmt, S. Linse, and M. D. Fayer, Photophysics of Polymer Systems, ACS Symposium Book Series (1986).

97. "Gas Phase Dynamics and Spectroscopy Probed with Picosecond Transient Grating Experiments," Todd S. Rose, William L. Wilson, G. Wäckerle, and M. D. Fayer, J. Chem. Phys., submitted (1986).

*Work supported by DOE under previous contracts and grants.

**Work suported by DOE under the current grant.

END

DATE FILMED

01/02/92